Eur. Phys. J. C 51, 37–53 (2007)
DOI 10.1140/epjc/s10052-007-0275-x

THE EUROPEAN PHYSICAL JOURNAL C

Regular Article – Theoretical Physics

Weak interaction effects in top-quark pair production at hadron colliders

J.H. Kühn[1], A. Scharf[1], P. Uwer[2,a,b]

[1] Institut für Theoretische Teilchenphysik, Universität Karlsruhe, Postfach 6980, 76128 Karlsruhe, Germany
[2] CERN, Department of Physics, Theory Unit, 1211 Geneva 23, Switzerland

Received: 10 November 2006 / Revised version: 7 February 2007 /
Published online: 5 April 2007 –

Abstract. Top-quark physics plays an important role at hadron colliders such as the Tevatron at Fermilab or the upcoming Large Hadron Collider (LHC) at CERN. Given the planned experimental precision, detailed theoretical predictions are mandatory. In this article we present analytic results for the complete weak corrections to gluon-induced top-quark pair production – neglecting purely photonic corrections, completing our earlier results for the quark-induced reaction. As an application we discuss top-quark pair production at the Tevatron and LHC. In particular we show that, although they are small for inclusive quantities, weak corrections can be sizeable for differential distributions.

1 Introduction

Top-quark physics plays an important role at the Tevatron and will be an equally important topic at the upcoming LHC. In view of the large production rate, amounting to $\mathcal{O}(10^8)$ top-quark pairs for an integrated luminosity of $200\,\mathrm{fb}^{-1}$, precise and direct measurements will be possible, which require a similarly detailed theoretical understanding of these reactions. Both single top-quark production and top-quark pair production have been studied extensively in the past. The differential cross section for top-quark pair production is known to next-to-leading order (NLO) accuracy in quantum chromodynamics (QCD) [1–5]. In addition, the resummation of logarithmic enhanced contributions has been studied in detail in [6–11]. Recently also the spin correlations between the top-quark and antitop-quark were calculated at NLO accuracy in QCD [5, 12].

Although formally suppressed through the small coupling, weak corrections can also be significant because of the presence of large Sudakov logarithms (see e.g. [13–16] and references therein), which were also studied in the context of γ and Z production at hadron colliders [17–19]. The origin of these large logarithms is easily understood: at high scale the massive gauge bosons W and Z behave essentially like massless bosons. Collinear and soft phenomena thus lead to large negative corrections. In strictly massless theories like QED or QCD these contributions are canceled through similar positive terms from the real corrections. This cancelation does not take place in the case of weak interactions, because the real and virtual emissions lead to different experimental signatures. Given that top-quark pair production at high scale is an ideal tool to search for new physics, it is clear that the precise knowledge of the weak corrections in this region is of paramount importance. In [20] weak corrections to top-quark pair production in hadronic collisions were investigated for the first time. More precisely, the partonic subprocesses $q\bar{q} \to t\bar{t}$ and $gg \to t\bar{t}$ were studied. In a subsequent study [21] parity-violating asymmetries were analysed in a two-Higgs doublet model and the minimal supersymmetric standard model.

In the original works some contributions were omitted. For the quark–antiquark-initiated process the gluon–Z box contributions (Fig. 1a) and the corresponding real corrections (Fig. 1b) are missing in [20]. They were recently evaluated in [22, 23]. For the gluon-fusion process a class of contributions related to triangle diagrams (Fig. 1c) are missing in [20], as noted also in [24], where the calculation of [20] has been repeated for the gluon-induced top-quark pair production. In [24] no analytic results are presented. In view of the importance of the analysis for upcoming experiments it is the purpose of this paper to repeat the original calculation [20] – including all missing contributions – and present compact analytic results well suited for the experimental analysis.

The outline of the paper is as follows: in Sect. 2 we present the calculation of the virtual weak corrections to top-quark pair production through gluon fusion – neglecting purely photonic corrections. In the gluon-fusion channel there are no real corrections from gluon emission contributing to the weak corrections – different from the $q\bar{q}$-channel [22]. The virtual corrections are thus infrared-finite and represent the complete weak corrections for this channel. Compact analytic expressions in terms of scalar

[a] e-mail: Peter.Uwer@cern.ch
[b] Heisenberg fellow

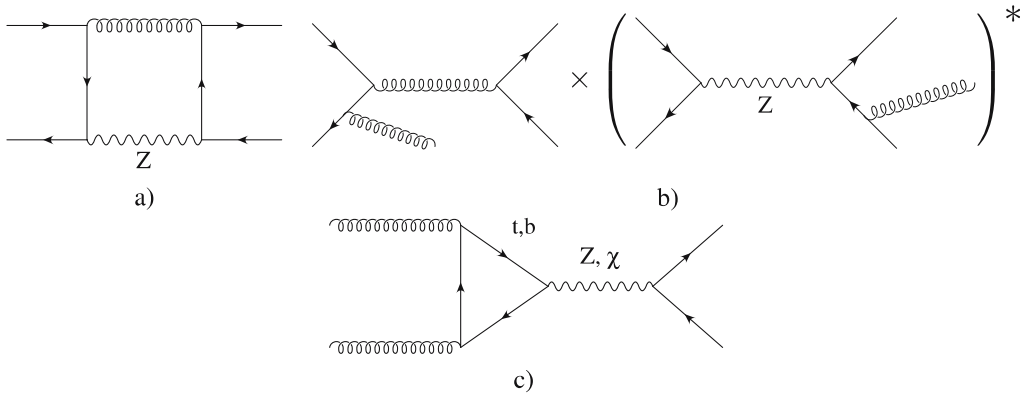

Fig. 1. Pictorial representation of contributions missing in [20]

one-loop integrals are given in Sect. 2 and in the appendix. In Sect. 3 we present numerical results for the gluon-fusion process at the parton level. Furthermore we combine the gluon channel with the quark–antiquark annihilation process (with the weak corrections taken from [22]), fold them with parton distributions, and give results for the corrections to the total cross section and to transverse momentum and top–antitop invariant mass distributions relevant for the Tevatron and the LHC.

2 Weak corrections to gluon fusion

To set up our notation we start with the QCD tree-level contribution. The three contributions to the amplitude are shown in Fig. 2. Evaluating the Feynman diagrams we obtain the well-known leading order differential cross section:

$$\frac{\mathrm{d}\sigma_{\mathrm{LO}}}{\mathrm{d}z} = \sigma_0 \frac{N^2(1+\beta^2 z^2)-2}{N(1-\beta^2 z^2)^2} \times (1-\beta^4 z^4 + 2\beta^2(1-\beta^2)(1-z^2)), \qquad (1)$$

where N is the number of colors, α_{s} the strong coupling constant, and β the velocity of the top-quark in the partonic center-of-mass system:

$$\beta = \sqrt{1-\frac{4m_t^2}{s}} \qquad (2)$$

(s denotes the partonic center-of-mass energy squared). The cosine of the scattering angle is denoted by z. Here and in what follows it is convenient to use the abbreviation

$$\sigma_0 = \frac{\pi\alpha_{\mathrm{s}}^2}{4}\frac{1}{N^2-1}\frac{\beta}{s}. \qquad (3)$$

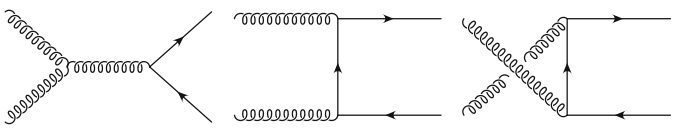

Fig. 2. Born diagrams for top-quark pair production via gluon fusion

A factor $1/(4(N^2-1)^2)$ from averaging over the incoming spins and color is included in the above result.

For the calculation of the weak corrections we use the 't Hooft–Feynman gauge (R_ξ gauge) with the gauge parameters ξ^i set to 1. The longitudinal degrees of freedom of the massive gauge bosons Z and W are thus represented by the Goldstone fields χ and ϕ. Ghost fields do not contribute at the order under consideration. Sample diagrams are shown in Fig. 3. The Cabibbo–Kobayashi–Maskawa mixing matrix is set to 1.

Before presenting the results for the weak corrections, let us add a few technical remarks. We use the Passarino–Veltman reduction scheme [25] to reduce analytically the tensor integrals to scalar integrals. For these the following

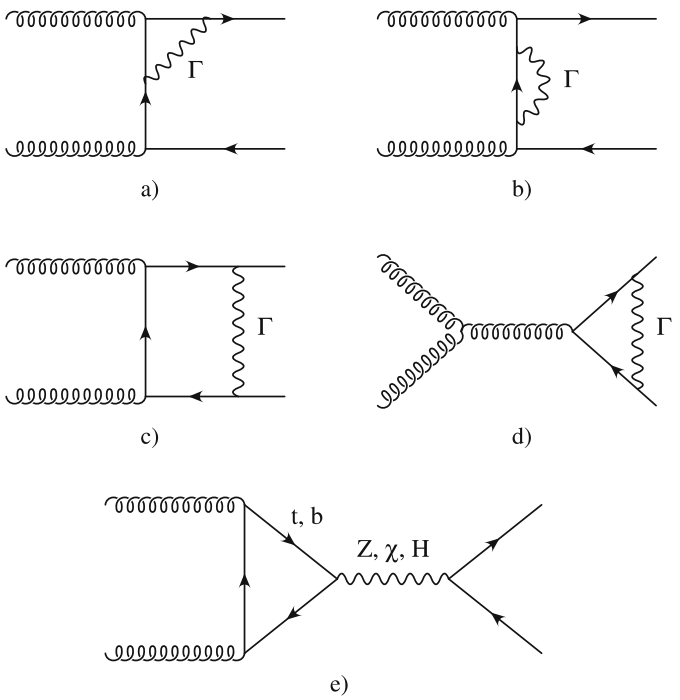

Fig. 3. Sample diagrams for the virtual corrections; Γ stands for all contributions from gauge boson, Goldstone boson and Higgs exchange

convention is used:

$$X_0 = \frac{1}{\mathrm{i}\pi^2}\int \mathrm{d}^d\ell \frac{(2\pi\mu)^{2\varepsilon}}{\left(\ell^2 - m_1^2 + \mathrm{i}\epsilon\right)\cdots}. \tag{4}$$

For the UV-divergent integrals we define the finite part for the one-point integrals A_0 and the two-point integrals B_0 through

$$\begin{aligned} A_0(m^2) &= m^2\Delta + \overline{A}_0(m^2)\,, \\ B_0\left(p^2, m_1^2, m_2^2\right) &= \Delta + \overline{B}_0\left(p^2, m_1^2, m_2^2\right), \end{aligned} \tag{5}$$

with $\Delta = 1/\varepsilon - \gamma + \ln(4\pi)$. The renormalization is performed in the counterterm formalism, where the bare Lagrangian $\mathcal{L}$ is rewritten in terms of renormalized fields and couplings:

$$\begin{aligned} \mathcal{L}(\Psi_0, A_0, m_0, g_0) &= \mathcal{L}\left(Z_\Psi^{1/2}\Psi_\mathrm{R}, Z_A^{1/2}A_\mathrm{R}, Z_m m_\mathrm{R}, Z_g g_\mathrm{R}\right) \\ &\equiv \mathcal{L}(\Psi_\mathrm{R}, A_\mathrm{R}, m_\mathrm{R}, g_\mathrm{R}) \\ &\quad + \mathcal{L}_\mathrm{ct}(\Psi_\mathrm{R}, A_\mathrm{R}, m_\mathrm{R}, g_\mathrm{R})\,. \end{aligned} \tag{6}$$

The contribution $\mathcal{L}(\Psi_\mathrm{R}, A_\mathrm{R}, m_\mathrm{R}, g_\mathrm{R})$ gives just the ordinary Feynman rules, but with the bare couplings replaced by the renormalized ones. The complete list of Feynman rules can be found, for example, in [26]. The contribution $\mathcal{L}_\mathrm{ct}(\Psi_\mathrm{R}, A_\mathrm{R}, m_\mathrm{R}, g_\mathrm{R})$ in (6) yields the counterterms, which render the calculation ultraviolet finite. Some of the resulting diagrams are shown in Fig. 4. For the present calculation, only wave function and mass renormalization are needed. No coupling constant renormalization has to be performed. This is a consequence of the fact that, although the weak corrections appear as a loop correction, they are still leading order in the weak couplings. Mass and wave function renormalizations are performed in the on-shell scheme:

$$m_{t,0} = m_t + \delta m_t\,, \tag{7}$$

$$\Psi_{t,0}^{\mathrm{R,L}} = \left(Z_t^{\mathrm{R,L}}\right)^{1/2}\Psi_t^{\mathrm{R,L}} = \left(1 + \frac{1}{2}\delta Z_t^{\mathrm{R,L}}\right)\Psi_t^{\mathrm{R,L}}. \tag{8}$$

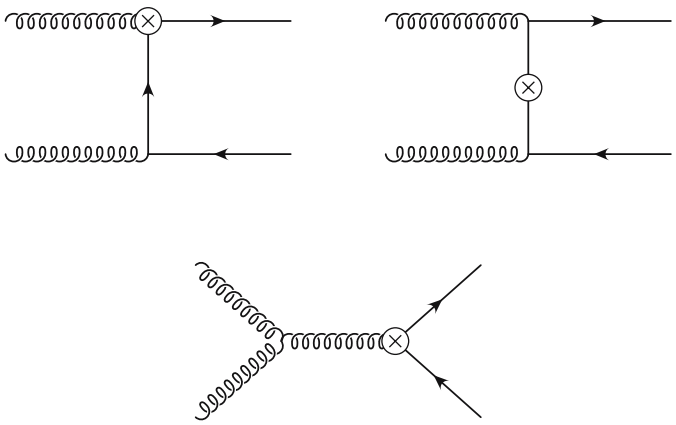

Fig. 4. Sample counterterm diagrams

The renormalization constants are thus given in terms of self-energy corrections Σ and their derivatives:

$$\begin{aligned} \delta Z_\mathrm{V} &= \frac{1}{2}\left(\delta Z_t^\mathrm{L} + \delta Z_t^\mathrm{R}\right) \\ &\quad = -\Sigma_\mathrm{V}\left(p^2 = m_t^2\right) - 2m_t^2\,\frac{\partial}{\partial p^2}(\Sigma_\mathrm{V} + \Sigma_\mathrm{S})\bigg|_{p^2=m_t^2}\,, \\ \delta Z_\mathrm{A} &= \frac{1}{2}\left(\delta Z_t^\mathrm{L} - \delta Z_t^\mathrm{R}\right) = -\Sigma_\mathrm{A}\left(p^2 = m_t^2\right), \\ \frac{\delta m_t}{m_t} &= -\Sigma_\mathrm{V}\left(p^2 = m_t^2\right) - \Sigma_\mathrm{S}\left(p^2 = m_t^2\right). \end{aligned} \tag{9}$$

The functions $\Sigma_{\mathrm{V,A,S}}$ can be found for example in [26]. Here we need only δZ_V and $\delta m_t/m_t$. Their explicit form in terms of scalar integrals – using the notation of this paper – reads

$$\begin{aligned} \delta Z_\mathrm{V} = \frac{\alpha}{4\pi}\Bigg\{\Bigg[& g_\mathrm{v}^{t\,2} + g_\mathrm{a}^{t\,2} \\ & + \frac{1}{m_t^2}\left(g_\mathrm{v}^{t\,2} + g_\mathrm{a}^{t\,2}\right)\left(A_0\left(m_Z^2\right) - A_0\left(m_t^2\right) - m_Z^2 B_0^Z\right) \\ & + \left(2\left(g_\mathrm{v}^{t\,2} + g_\mathrm{a}^{t\,2}\right)m_Z^2 + 4m_t^2\left(g_\mathrm{v}^{t\,2} - 3g_\mathrm{a}^{t\,2}\right)\right) \\ & \times \frac{\mathrm{d}}{\mathrm{d}p^2}B_0^Z\bigg|_{p^2=mt^2}\Bigg] \\ & + \frac{1}{2s_\mathrm{W}^2}\Bigg[\frac{1}{2} + \frac{1}{2m_t^2}\left(A_0\left(m_\mathrm{W}^2\right) - A_0\left(m_b^2\right)\right) \\ & - \frac{m_t^2 - m_b^2 + m_\mathrm{W}^2}{2m_t^2}B_0^W \\ & - \left(m_t^2 - m_\mathrm{W}^2 + m_b^2\right)\,\frac{\mathrm{d}}{\mathrm{d}p^2}B_0^W\bigg|_{p^2=mt^2}\Bigg] \\ & + \frac{m_t^2}{4s_\mathrm{W}^2 m_\mathrm{W}^2}\Bigg[\frac{1}{2m_t^2}\left(A_0\left(m_Z^2\right) - A_0\left(m_t^2\right) - m_Z^2 B_0^Z\right) \\ & + m_Z^2\,\frac{\mathrm{d}}{\mathrm{d}p^2}B_0^Z\bigg|_{p^2=mt^2}\Bigg] \\ & + \frac{1}{2s_\mathrm{W}^2}\frac{1}{4m_\mathrm{W}^2}\Bigg[\frac{m_t^2 + m_b^2}{m_t^2}\left(A_0\left(m_\mathrm{W}^2\right) - A_0\left(m_b^2\right)\right) \\ & - \frac{\left(m_t^2 - m_b^2 + m_\mathrm{W}^2\right)\left(m_t^2 + m_b^2\right)}{m_t^2}B_0^W \\ & - 2\left(\left(m_t^2 - m_b^2\right)^2 - m_\mathrm{W}^2\left(m_t^2 + m_b^2\right)\right)\frac{\mathrm{d}}{\mathrm{d}p^2}B_0^W\bigg|_{p^2=mt^2}\Bigg] \\ & + \frac{m_t^2}{4s_\mathrm{W}^2 m_\mathrm{W}^2}\Bigg[\frac{1}{2m_t^2}\left(A_0\left(m_H^2\right) - A_0\left(m_t^2\right) - m_H^2 B_0^H\right) \\ & - \left(4m_t^2 - m_H^2\right)\,\frac{\mathrm{d}}{\mathrm{d}p^2}B_0^H\bigg|_{p^2=mt^2}\Bigg]\Bigg\}\,, \end{aligned} \tag{10}$$

$$\begin{aligned} \frac{\delta m_t}{m_t} = -\frac{\alpha}{4\pi}\Bigg\{ & \frac{1}{m_t^2}\Big[\left(3g_\mathrm{a}^{t\,2} - g_\mathrm{v}^{t\,2}\right)m_t^2 \\ & + \left(g_\mathrm{v}^{t\,2} + g_\mathrm{a}^{t\,2}\right)\left(A_0\left(m_t^2\right) - A_0\left(m_Z^2\right)\right) \\ & + \left(\left(g_\mathrm{v}^{t\,2} + g_\mathrm{a}^{t\,2}\right)m_Z^2 + 2m_t^2\left(g_\mathrm{v}^{t\,2} - 3g_\mathrm{a}^{t\,2}\right)\right)B_0^Z\Big] \\ & + \frac{1}{4s_\mathrm{W}^2 m_t^2}\Big[m_t^2 + \left(A_0\left(m_b^2\right) - A_0\left(m_\mathrm{W}^2\right)\right) \end{aligned}$$

$$
\begin{aligned}
&+\left(m_{\mathrm{W}}^2-m_b^2-m_t^2\right)B_0^W\big]\\
&+\frac{1}{8s_{\mathrm{W}}^2m_{\mathrm{W}}^2}\left[A_0\left(m_t^2\right)-A_0\left(m_Z^2\right)+m_Z^2B_0^Z\right]\\
&+\frac{1}{8s_{\mathrm{W}}^2m_{\mathrm{W}}^2m_t^2}\big[\left(m_t^2+m_b^2\right)\left(A_0\left(m_b^2\right)-A_0\left(m_{\mathrm{W}}^2\right)\right)\\
&-\left(\left(m_t^2-m_b^2\right)^2-m_{\mathrm{W}}^2\left(m_t^2+m_b^2\right)\right)B_0^W\big]\\
&+\frac{1}{8s_{\mathrm{W}}^2m_{\mathrm{W}}^2}\big[A_0\left(m_t^2\right)-A_0\left(m_H^2\right)\\
&+\left(m_H^2-4m_t^2\right)B_0^H\big]\Bigg\}, \qquad (11)
\end{aligned}
$$

where s_{W} (c_{W}) denotes the sine (cosine) of the weak mixing angle. The vector (g_{v}^t) and axial-vector (g_{a}^t) couplings of the top-quark to the Z boson are given in terms of the weak isospin T_3^f and the electric charge Q_f for a fermion of flavor f:

$$g_{\mathrm{v}}^f=\frac{1}{2s_{\mathrm{W}}c_{\mathrm{W}}}\left(T_3^f-2s_{\mathrm{W}}^2Q_f\right), \qquad (12)$$

$$g_{\mathrm{a}}^f=\frac{1}{2s_{\mathrm{W}}c_{\mathrm{W}}}T_3^f. \qquad (13)$$

The coupling of the top-quark to the W boson is given by

$$g_{\mathrm{W}}=\frac{1}{2\sqrt{2}s_{\mathrm{W}}}. \qquad (14)$$

As usual α stands for the fine structure constant, which will be taken as running coupling evaluated at the scale $2m_t$. The mass of particle i is denoted by m_i. The abbreviations $B_0^{Z,W,H}$ for the two-point scalar loop integrals are defined in the appendix. Note that the photonic corrections form a gauge-independent subset and are not included in (10) and (11) or in the following discussion.

For the following discussion it is convenient to separate the weak corrections into the contribution from vertex diagrams (t-, u-, s-channel, Fig. 3a and d), self-energy diagrams (Fig. 3b) and box diagrams (Fig. 3c). The triangle diagrams in Fig. 3e are finite without renormalization and will be studied separately. The differential cross section at next-to-leading order is decomposed as follows:

$$
\begin{aligned}
\frac{\mathrm{d}\sigma^{\mathrm{NLO}}}{\mathrm{d}z}=&\sum_{i=Z,W,\chi,\phi,H}\frac{\mathrm{d}\sigma_i^{\square}}{\mathrm{d}z}+\frac{\mathrm{d}\sigma_i^{\mathrm{V}}}{\mathrm{d}z}+\frac{\mathrm{d}\sigma_i^{s\mathrm{V}}}{\mathrm{d}z}+\frac{\mathrm{d}\sigma_i^{\Sigma}}{\mathrm{d}z}\\
&+\sum_{i=Z,\chi,H}\frac{\mathrm{d}\sigma_i^{\triangle}}{\mathrm{d}z}. \qquad (15)
\end{aligned}
$$

We start with the analytic results for the triangle diagrams. For the Higgs and $(Z+\chi)$ terms we obtain

$$
\begin{aligned}
\frac{\mathrm{d}\sigma_H^{\triangle}}{\mathrm{d}z}=&\frac{\alpha}{\pi}\sigma_0\frac{m_t^2}{m_{\mathrm{W}}^2s_{\mathrm{W}}^2}\frac{\beta^2}{1-\beta^2z^2}\frac{1}{s-m_H^2}\\
&\times\left[m_t^2(s-4m_t^2)C_0^t+m_b^2(s-4m_b^2)C_0^b\right.\\
&\left.-2(m_t^2+m_b^2)\right], \qquad (16)
\end{aligned}
$$

$$\frac{\mathrm{d}\sigma_{Z+\chi}^{\triangle}}{\mathrm{d}z}=16\frac{\alpha}{\pi}\sigma_0g_{\mathrm{a}}^t\frac{m_t^2}{m_Z^2(1-\beta^2z^2)}\left(g_{\mathrm{a}}^tm_t^2C_0^t+g_a^bm_b^2C_0^b\right). \qquad (17)$$

A factor $1/(4(N^2-1)^2)$ from averaging over the incoming spins and color is again included. The integrals $C_0^{b,t}$ are defined in the appendix. As a consequence of Furry's theorem only the axial-vector-induced terms contribute in the case where the Z boson appears in the s-channel. Furthermore, the Landau–Yang theorem forbids the decay of an on-shell vector boson into two identical massless on-shell spin-one bosons. Therefore, the poles from the propagators of the Z boson and the χ are canceled in the $\sigma_{Z+\chi}^{\triangle}$ term, as is evident from (17).

For the remaining vertex corrections with a gluon in the s-channel, we obtain

$$
\begin{aligned}
\frac{\mathrm{d}\sigma_Z^{s\mathrm{V}}}{\mathrm{d}z}=&-2\frac{\alpha}{\pi}\sigma_0N\frac{m_t^2}{s^2}\frac{z^2}{1-\beta^2z^2}\\
&\times\Bigg\{2\left[2\left(g_{\mathrm{v}}^{t\,2}+g_{\mathrm{a}}^{t\,2}\right)m_Z^2-s\beta^2\left(g_{\mathrm{v}}^{t\,2}-3g_{\mathrm{a}}^{t\,2}\right)\right]\\
&\times\left(\overline{B}_0^t-\overline{B}_0^Z\right)\\
&+\left[4\left(g_{\mathrm{v}}^{t\,2}+g_{\mathrm{a}}^{t\,2}\right)m_Z^4+8g_{\mathrm{a}}^{t\,2}m_Z^2s\beta^2\right.\\
&-s^2\beta^2\left(g_{\mathrm{v}}^{t\,2}+g_{\mathrm{a}}^{t\,2}+\beta^2\left(g_{\mathrm{v}}^{t\,2}-3g_{\mathrm{a}}^{t\,2}\right)\right)\big]C_0^Z\\
&+s\beta^2\big[2m_Z^2\left(g_{\mathrm{v}}^{t\,2}+g_{\mathrm{a}}^{t\,2}\right)\\
&\left.+s(1-\beta^2)\left(g_{\mathrm{v}}^{t\,2}-3g_{\mathrm{a}}^{t\,2}\right)\big]\frac{\mathrm{d}}{\mathrm{d}p^2}B_0^Z\right|_{p^2=mt^2}\Bigg\}, \qquad (18)\\
\frac{\mathrm{d}\sigma_W^{s\mathrm{V}}}{\mathrm{d}z}=&-8\frac{\alpha}{\pi}\sigma_0g_{\mathrm{W}}^2N\frac{m_t^2}{s^2}\frac{z^2}{1-\beta^2z^2}\\
&\times\Bigg\{\frac{1}{2}\left(s(1+\beta^2)+4\left(m_{\mathrm{W}}^2-m_b^2\right)\right)\left(\overline{B}_0^b-\overline{B}_0^W\right)\\
&+\frac{1}{8}\left(\left(s(1+\beta^2)+4\left(m_{\mathrm{W}}^2-m_b^2\right)\right)^2-4\beta^2s^2\right)C_0^W\\
&-\frac{1}{4}s\beta^2\left(s(1-\beta^2)+4\left(m_b^2-m_{\mathrm{W}}^2\right)\right)\\
&\times\left.\frac{\mathrm{d}}{\mathrm{d}p^2}B_0^W\right|_{p^2=mt^2}\Bigg\}, \qquad (19)\\
\frac{\mathrm{d}\sigma_\chi^{s\mathrm{V}}}{\mathrm{d}z}=&-8\frac{\alpha}{\pi}\sigma_0g_{\mathrm{a}}^{t\,2}N\frac{m_t^4}{s^2}\frac{z^2}{1-\beta^2z^2}\\
&\times\Bigg\{2\left(\overline{B}_0^t-\overline{B}_0^Z\right)+\left(2m_Z^2+s\beta^2\right)C_0^Z\\
&\left.+s\beta^2\left.\frac{\mathrm{d}}{\mathrm{d}p^2}B_0^Z\right|_{p^2=mt^2}\right\}, \qquad (20)\\
\frac{\mathrm{d}\sigma_\phi^{s\mathrm{V}}}{\mathrm{d}z}=&-8\frac{\alpha}{\pi}\sigma_0\frac{g_{\mathrm{W}}^2}{m_{\mathrm{W}}^2}N\frac{m_t^2}{s^2}\frac{z^2}{1-\beta^2z^2}\\
&\times\Bigg\{\frac{1}{16}\left(16m_b^4+m_b^2\left(8s\beta^2-16m_{\mathrm{W}}^2\right)\right.\\
&\left.-4m_{\mathrm{W}}^2s(1-\beta^2)-s^2(1-\beta^4)\right)\left(\overline{B}_0^W-\overline{B}_0^b\right)\\
&+\frac{1}{64}\big[64m_b^6-16m_b^4\left(8m_{\mathrm{W}}^2+s(1-\beta^2)\right)\\
&+16m_{\mathrm{W}}^4s(1-\beta^2)+4m_b^2\left(16m_{\mathrm{W}}^4-s^2(1-\beta^2)^2\right)\\
&+8m_{\mathrm{W}}^2s^2(1-\beta^4)+s^3(1-\beta^2)^3\big]C_0^W\\
&-\frac{1}{32}\big[16m_b^4s\beta^2-8m_b^2\left(2m_{\mathrm{W}}^2s\beta^2+s^2\beta^2(1-\beta^2)\right)
\end{aligned}
$$

$$
\begin{aligned}
&- 4m_{\rm W}^2 s^2\beta^2(1-\beta^2) + s^3\beta^2(1-\beta^2)^2\big] \\
&\times \frac{\mathrm{d}}{\mathrm{d}p^2} B_0^W\Big|_{p^2=mt^2} \Big\}, \qquad (21)\\
\frac{\mathrm{d}\sigma_H^{s\mathrm{V}}}{\mathrm{d}z} &= 4\frac{\alpha}{\pi}\sigma_0 g_{\rm W}^2 N \frac{m_t^2}{s^2}\frac{z^2}{1-\beta^2 z^2}\frac{m_t^2}{m_{\rm W}^2} \\
&\times \Big\{ 2\big(s\beta^2 + m_H^2\big)\big(\overline{B}_0^H - \overline{B}_0^t\big) \\
&+ \big(s^2\beta^2(1-\beta^2) - 3m_H^2 s\beta^2 - 2m_H^4\big) C_0^H \\
&+ s\beta^2\big(s(1-\beta^2) - m_H^2\big)\ \frac{\mathrm{d}}{\mathrm{d}p^2} B_0^H\Big|_{p^2=mt^2} \Big\}. \qquad (22)
\end{aligned}
$$

The remaining contributions to the differential cross section are listed in Appendix B.

Before showing concrete results for hadron colliders we discuss several checks of our result. We performed two independent calculations yielding also two independent numerical computer codes. We checked that we obtain the correct structure for the UV singularities yielding a finite result after renormalization. In our notation this corresponds to a stringent test of the coefficients of the A_0 and B_0 integrals. The behavior of the Higgs corrections close to threshold and for light Higgs bosons is well understood (see for example [27] and references therein). This allows us to test the Higgs contributions for a very light Higgs near threshold. For a $t\bar{t}$ system produced through a vector current, the Higgs correction is given by the factor $(1 + H_{\rm thr}(r))$ with

$$
\begin{aligned}
H_{\rm thr}(r) = \frac{2\kappa}{\pi}\Big\{ &- \frac{1}{12}\Big[-12 + 4r + (-12 + 9r - 2r^2)\ln(r) \\
&+ \frac{2}{r}(-6 + 5r - 2r^2)\sqrt{r(4-r)}\arccos\left(\frac{\sqrt{r}}{2}\right)\Big] \\
&- \frac{\pi}{\sqrt{r}} + \frac{\pi}{2\beta}\arctan\left(\frac{2\beta}{\sqrt{r}}\right)\Big\} \qquad (23)
\end{aligned}
$$

and

$$
r = \frac{m_H^2}{m_t^2}\,, \qquad \kappa = \frac{\alpha}{4}\frac{m_t^2}{s_{\rm W}^2 m_{\rm W}^2}\,. \qquad (24)
$$

In Fig. 5 we show the numerical result for $m_H = 0.1\,\mathrm{MeV}$ as a function of the variable η defined through

$$
\eta = \frac{s}{4m_t^2} - 1. \qquad (25)
$$

The line shows the Higgs contribution according to (23). The crosses show the result from the full Higgs-boson-induced correction. The enhancement proportional to $1/\beta$ is well recovered by the calculation. The numerical agreement is between four ($\eta = 10^{-5}$) and two digits ($\eta = 10^{-3}$). As we shall see later, the enhancement close to threshold for a light Higgs can still be observed even for a Higgs mass of 120 GeV, although reduced to 2%. A similar test has been performed for a light Z boson. Again we find perfect agreement. In addition we compared analytically the results for the t- and u-channel vertices, self-energies and Higgs triangle diagrams with those from [20]. We find complete agreement, after the correction of some typos in [20]. Using the same input parameters we also compared the plots shown in [20] and found agreement. Finally, we compared our results numerically with those of [28] and found perfect agreement. However, we are in disagreement with the results published recently in [24]. In particular, for the transverse momentum and top–antitop invariant mass distribution we find negative corrections close to threshold, while the corrections are positive in [24] (Fig. 1). Our findings are also confirmed in [28].

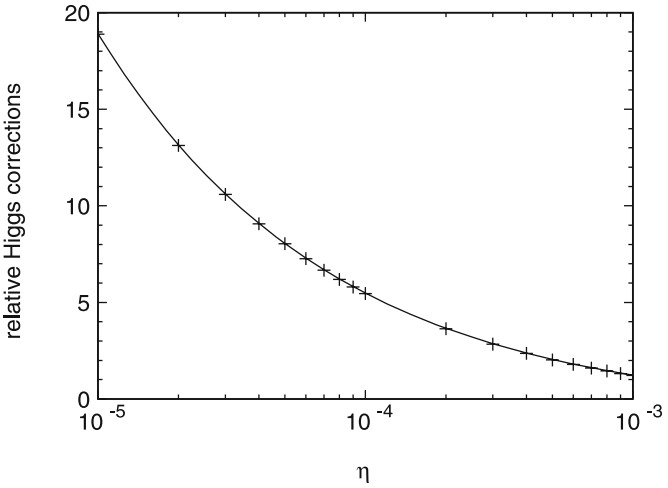

Fig. 5. Comparison of the full corrections from Higgs boson exchange with the corrections based on (23) ($m_H = 0.1\,\mathrm{MeV}$)

3 Numerical results

In this section we present numerical results for the gluon-fusion process at order $\alpha_{\rm s}^2\alpha$. We use the following coupling constants:

$$
\alpha(2m_t) = \frac{1}{126.3}\,, \qquad \alpha_{\rm s} = 0.1\,,
$$

and, if not stated otherwise, the following masses:

$$
\begin{aligned}
m_Z &= 91.1876\,\mathrm{GeV}\,, & m_{\rm W} &= 80.425\,\mathrm{GeV}\,,\\
m_H &= 120\,\mathrm{GeV}\,, & & \\
m_b &= 4.82\,\mathrm{GeV}\,, & m_t &= 172.7\,\mathrm{GeV}\,.
\end{aligned}
$$

The weak mixing angle is fixed through the on-shell renormalization scheme used in the calculation.

In Fig. 6 the separate corrections as defined in (15) are shown at the parton level. We normalize the result to the leading-order $gg \to t\bar{t}$ process. The sum of the different contributions is shown as a solid line in Fig. 6. For moderate partonic energies the corrections are of the order of a few percent as might be expected for a weak correction. Near threshold the cross section is dominated by the triangle and the box diagrams. Both are of the same order of magnitude, but opposite in sign, leading to a significant

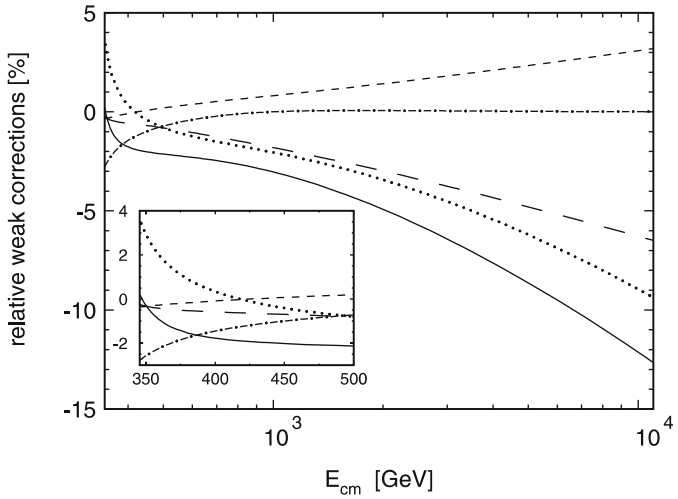

Fig. 6. Different contributions to the weak corrections: vertices (*long-dashed*), self-energies (*dashed*), boxes (*dotted*), triangles (*dash-dotted*). The sum is shown as the *full line*

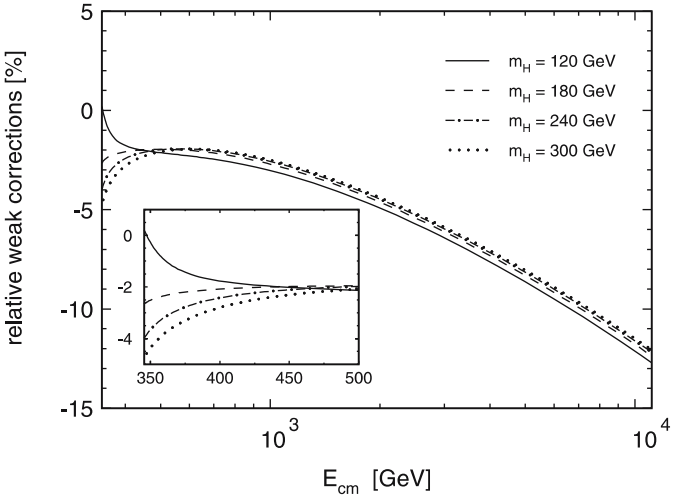

Fig. 8. The dependence of the partonic cross section from the Higgs mass: $m_H = 120\,\text{GeV}$ (*full line*), $m_H = 180\,\text{GeV}$ (*dashed*), $m_H = 240\,\text{GeV}$ (*dash-dotted*) and $m_H = 300\,\text{GeV}$ (*dotted*)

cancelation. It is worth noting at this point that the inclusion of the $(Z+\chi)$ triangle diagrams – neglected in [20] – decreases the result by about 2% in the threshold region ($m_H = 120\,\text{GeV}$). The $(Z+\chi)$ term dominates the triangle contributions. In Fig. 7 we illustrate the effect of $\sigma^{\triangle}_{Z+\chi}$ by comparing the full result with the result where $\sigma^{\triangle}_{Z+\chi}$ is neglected. Close to the threshold, the aforementioned 2% difference is observed. The $(Z+\chi)$ contribution accidentally compensates the positive contribution from Higgs exchange, which, however, becomes small, about 20 GeV above threshold. For energies above 600 GeV the contribution from the $(Z+\chi)$ triangle becomes negligible. The behavior of the box contribution close to the threshold, shown in Fig. 6, is a consequence of the Higgs effects discussed before.

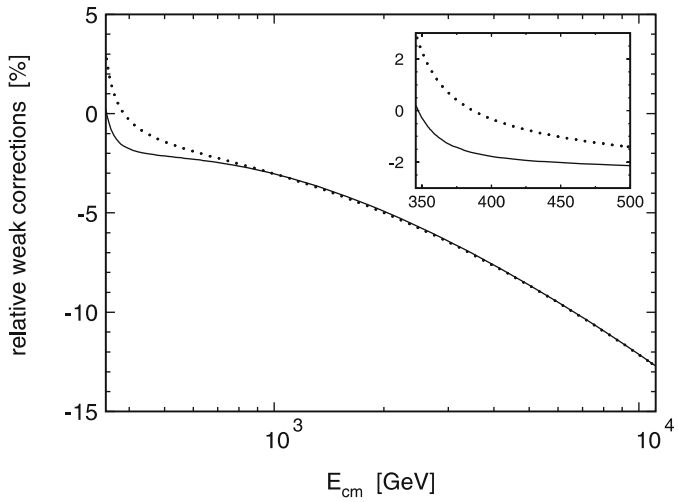

Fig. 7. Comparison between the weak corrections: with the Z and χ triangle diagrams included (*full*) and without these contributions (*dashed*)

On the other hand, for a partonic center-of-mass energy of around 500 GeV, the weak corrections start to become important and amount to more than 10% at a few TeV. If we compare the relative size of the weak correction for gluon- and quark–antiquark-induced reactions at large energies, we find that they are twice as large for the quark–antiquark process.

The dependence on the Higgs mass, i.e. the relative corrections for different Higgs masses, are shown in Fig. 8. The corrections are strongly dependent on m_H, with a variation of nearly 5% in the threshold region. Let us now address the effects of the weak corrections on hadronic observables. We used the parton distribution function CTEQ6L [29] evaluated at a factorization scale $\mu_\text{F} = 2m_t$. With the input mentioned before we obtain

$$\sigma^{\text{Tev}} = \sigma^{\text{Tev}}_{q\bar{q}} + \sigma^{\text{Tev}}_{gg} = 4.18\,\text{pb} + 0.19\,\text{pb} = 4.37\,\text{pb}$$

and

$$\sigma^{\text{LHC}} = \sigma^{\text{LHC}}_{q\bar{q}} + \sigma^{\text{LHC}}_{gg} = 56\,\text{pb} + 366\,\text{pb} = 422\,\text{pb}$$

for the leading-order cross section at the Tevatron and LHC, respectively. The leading-order estimate is significantly smaller than the QCD-corrected (NLO + resummation) result of about 6.7 pb for the Tevatron [11] and about 794 pb for the LHC [30]. To some extent the large QCD corrections are of universal character and it is plausible that the lowest order and electroweak corrected (total and differential) cross sections will be affected by similar corrections. Therefore we will, in the following, only present their relative size. In a first step we study the weak corrections to the total cross section at the Tevatron and the LHC as a function of m_t for three different Higgs masses (Fig. 9). The results include both quark–antiquark annihilation and gluon fusion. (We have also calculated the processes $qg \to t\bar{t}q$ and $\bar{q}g \to t\bar{t}\bar{q}$ at order $\alpha\alpha_\text{s}^2$. We find that

these contributions are tiny due to the missing Sudakov suppression. They are thus not included in the following discussion.)

As expected, the corrections to the inclusive cross section amount to a few percent only. Most of the top-quark pairs are produced close to threshold, where the weak corrections at parton level amount to a few percent only. The relative corrections are essentially given by the threshold behavior of the quark–antiquark channel for the Tevatron and the gluon channel for the LHC. The integrated cross section samples a wide range in the top–antitop invariant mass $M_{t\bar{t}}$ ($M_{t\bar{t}} = \sqrt{(k_t + k_{\bar{t}})^2}$), and the marked Higgs mass dependence of the partonic cross section close to threshold is washed out. The correction is nearly independent of the top-quark mass for values of m_t between 165 and 180 GeV. Given the experimental precision at the Tevatron and the LHC, it is unlikely that the weak corrections can be seen in the total cross section. Differential distributions in the transverse momentum p_{T} and top–antitop invariant mass $M_{t\bar{t}}$ are strongly affected, however. Indeed, the corrections to the $M_{t\bar{t}}$ distributions can be directly read off from Fig. 8, as far as the gluon-induced channel is concerned. Note that for the quark–antiquark process the situation is more involved, since real corrections are present [22]. In principle, it might be possible to establish the enhancement induced by the top-quark Yukawa coupling for a relatively light Higgs boson. However, the difference of 5% between a light (120 GeV) and a heavy (300 GeV) Higgs boson could be masked by QCD uncertainties, which are particularly large in the threshold region. Note that photonic corrections, which in principle could also lead to enhanced corrections in the threshold region due to the Coulomb singularity, are suppressed through the couplings. Furthermore the kinematic region in which the parametric suppression would be compensated by the $1/\beta$ behavior cannot be resolved experimentally at the LHC. In contrast, the weak corrections amount to more than 10% at high energy when the Sudakov suppression becomes also important. Therefore, we study their

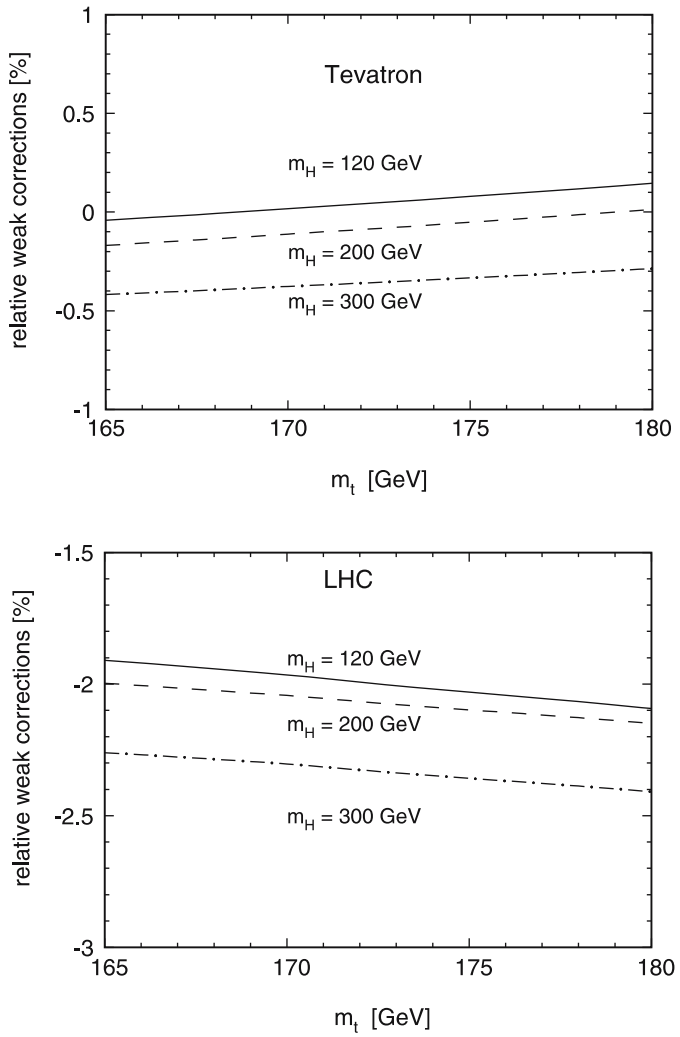

Fig. 9. Weak corrections to top-quark pair production at the Tevatron (*upper figure*) and the LHC (*lower figure*) for three different Higgs masses ($m_H = 120$ GeV (*full line*), $m_H = 200$ GeV (*dashed*), $m_H = 300$ GeV (*dash-dotted*))

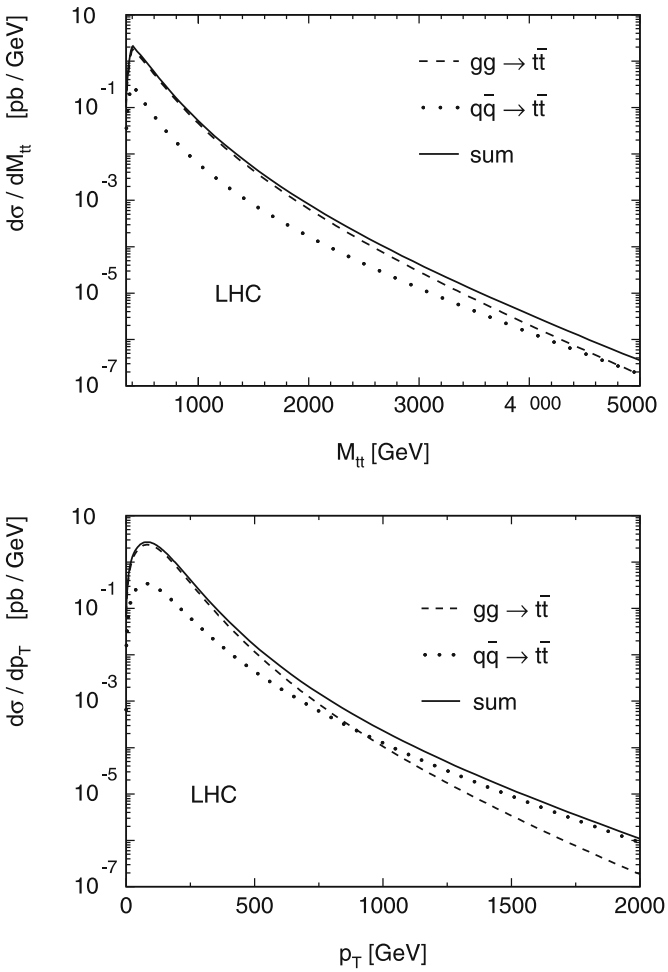

Fig. 10. Leading-order differential cross section for the LHC as a function of p_{T} and $M_{t\bar{t}}$. Shown is the sum (*full*) and the contributions from gluon fusion (*dashed*) and quark–antiquark annihilation (*dotted*)

effect on the differential distributions at large momentum transfer. The differential distribution in the top–antitop invariant mass $M_{t\bar{t}}$ being a sensitive tool in the search for new physics, this question is of particular importance. At large momentum transfer two competing effects must be considered: the increasing Sudakov logarithms, and the increasing statistical uncertainty.

To get a rough idea about the possible statistical sensitivity we show in Figs. 10 and 11 the leading-order differential cross sections in $M_{t\bar{t}}$ and p_{T}. For the LHC, about 10^8 events are expected for an integrated luminosity of $200\,\mathrm{fb}^{-1}$ and large values of $M_{t\bar{t}}$ and p_{T} will be accessible. An interesting behavior of the relative importance of gluon- versus quark-induced processes is observed for the LHC. For low $M_{t\bar{t}}$ and p_{T}, the gluon channel dominates. However, for p_{T} larger than 1 TeV the quark–antiquark annihilation process takes over, as a consequence of the change in relative importance of quark– antiquark with respect to gluon luminosities. For the Tevatron only the moderate values of 300 GeV for p_{T} and 700 GeV for $M_{t\bar{t}}$ are accessible at best. Furthermore, the quark–antiquark annihilation process dominates throughout.

The relative corrections of the differential distributions in p_{T} and $M_{t\bar{t}}$ are shown in Figs. 12 and 13 for the LHC and Tevatron. For large values of p_{T} and $M_{t\bar{t}}$, accessible at the LHC, sizeable negative corrections are predicted, reaching 10 to 15%. In contrast, the corrections are far smaller at the Tevatron. Taking $m_H = 120\,\mathrm{GeV}$, they are +3% close to threshold and −5% for $M_{t\bar{t}}$ around 800 GeV, leading to a distortion of the differential distribution by 8%. It remains to be seen whether QCD and experimental uncertainties can be pushed below this level. A rough guess of the statistical uncertainty expected for the LHC and Tevatron can be deduced from Figs. 14 and 15. The estimated number of events with $M_{t\bar{t}} \geq M_{t\bar{t}}^{\mathrm{cut}}$, based on a luminosity of $200\,\mathrm{fb}^{-1}$ for the LHC ($8\,\mathrm{fb}^{-1}$ for the Teva-

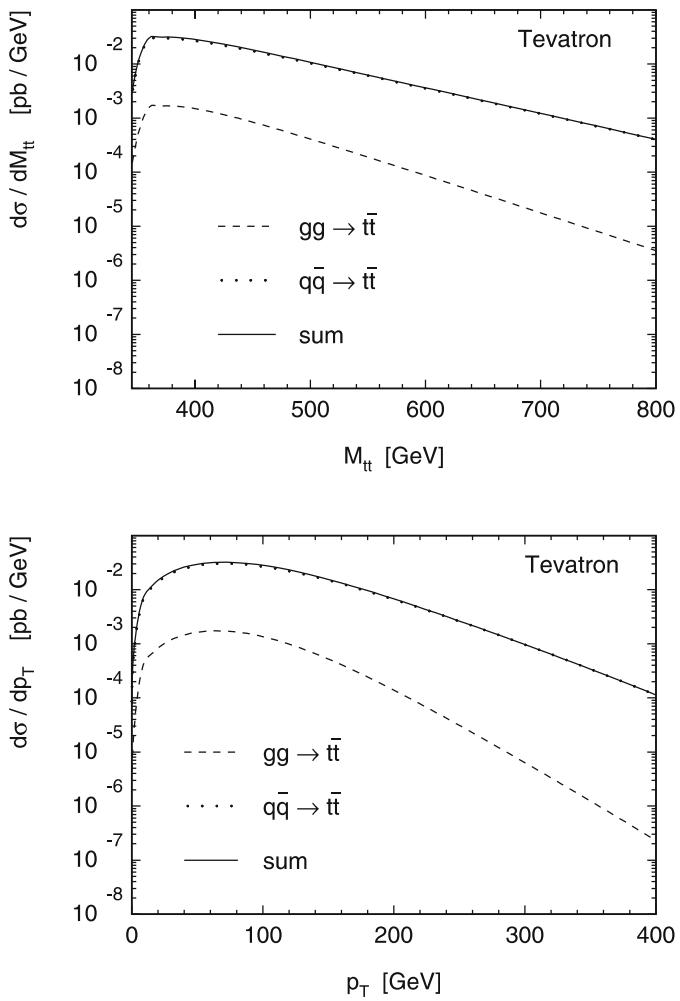

Fig. 11. Leading-order differential cross section for the Tevatron as a function of p_{T} and $M_{t\bar{t}}$. Shown is the sum (*full*) and the contributions from gluon fusion (*dashed*) and quark–antiquark annihilation (*dotted*)

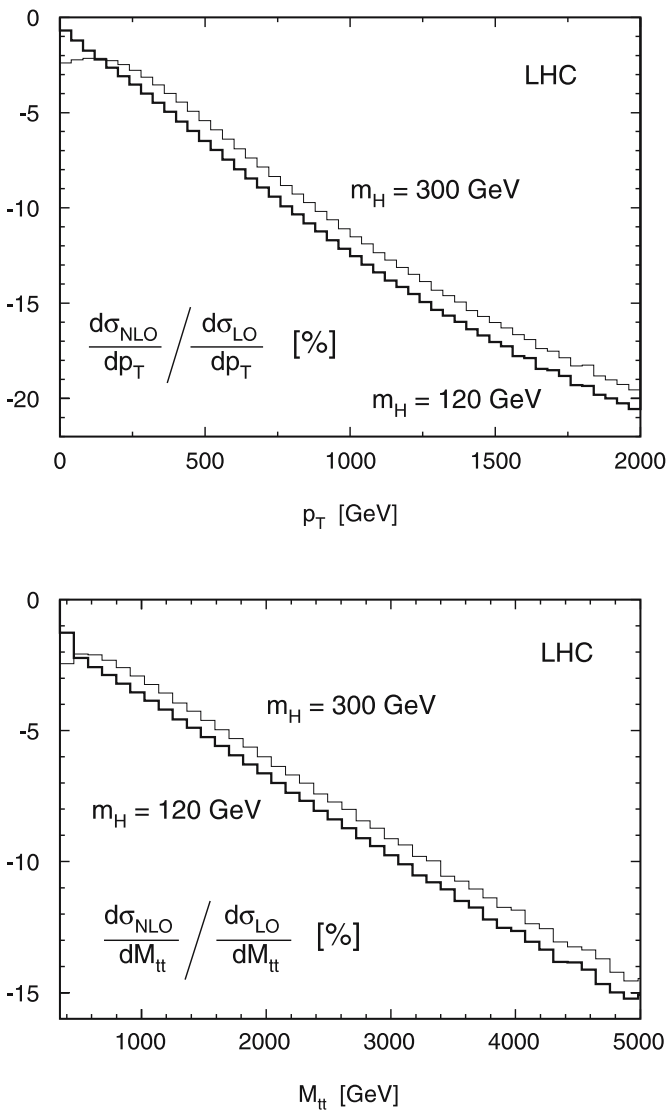

Fig. 12. The relative corrections to the p_{T} and $M_{t\bar{t}}$ distribution for the LHC for $m_H = 120\,\mathrm{GeV}$ (*bold histogram*) and $m_H = 300\,\mathrm{GeV}$ (*thin histogram*)

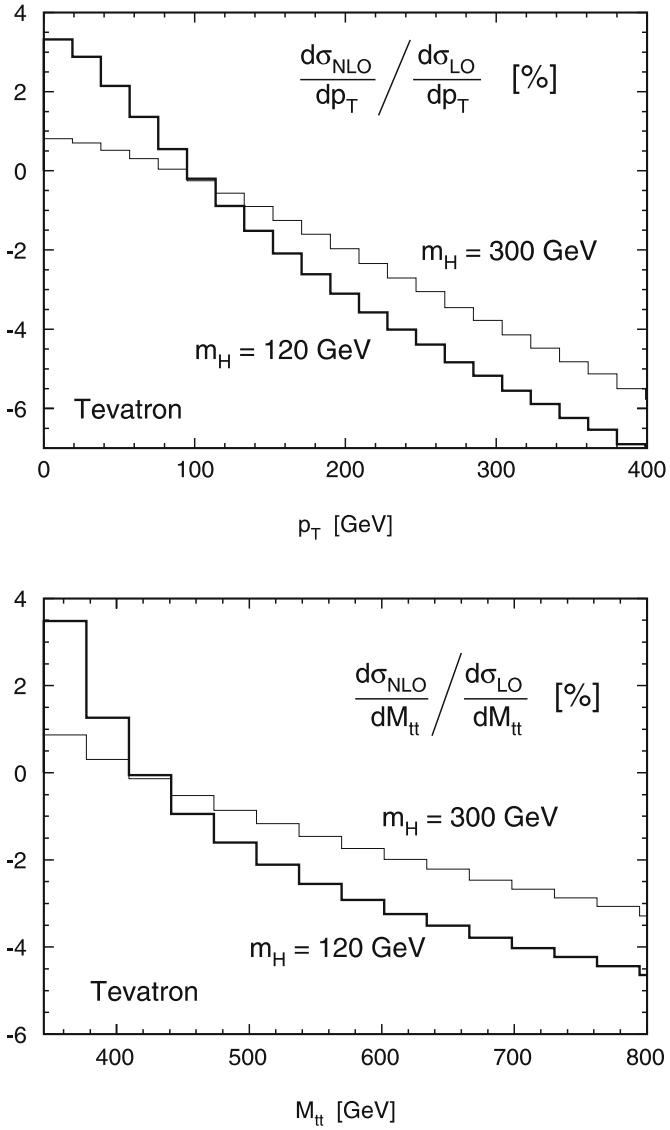

Fig. 13. The relative corrections to the p_{T} and $M_{t\bar{t}}$ distribution for the Tevatron for $m_H = 120\,\mathrm{GeV}$ (*bold histogram*) and $m_H = 300\,\mathrm{GeV}$ (*thin histogram*)

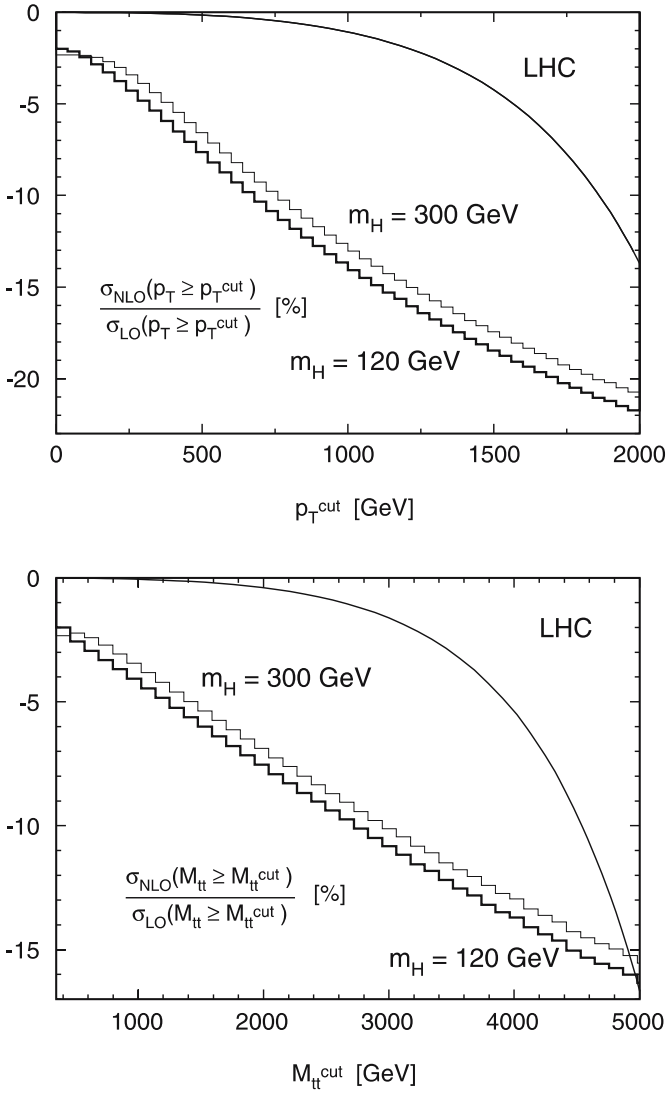

Fig. 14. The relative corrections to the p_{T} and $M_{t\bar{t}}$ distributions, integrated from a lower value in p_{T} and $M_{t\bar{t}}$ to the kinematic limit, for the LHC and two Higgs masses ($m_H = 120\,\mathrm{GeV}$ (*bold histogram*), $m_H = 300\,\mathrm{GeV}$ (*thin histogram*)). The *smooth curve* gives an estimate of the corresponding statistical uncertainty for an integrated luminosity of $200\,\mathrm{fb}^{-1}$

tron), is used to estimate the statistical uncertainty and compare it with the relative corrections, evaluated for the same sample. It will be difficult to observe the effect of the weak corrections at the Tevatron. At the LHC, with the large sample of top quarks, the statistical precision will match the size of the weak corrections, and eventually of the Higgs enhancement in the threshold region. Note that, although the results presented so far were only given for $\mu_{\mathrm{F}} = 2m_t$, we have also evaluated the corrections for $\mu_{\mathrm{F}} = m_t/2$. We find that the relative weak corrections are remarkable stable under the scale variation. The relative corrections change less than a few percent of their respective size. The residual scale dependence essentially cancels in the relative corrections between the numerator and the denominator.

Before closing this discussion, let us mention that also the dependence of the corrections on the bottom mass was investigated and the full dependence on the bottom-quark mass was kept throughout. Furthermore the results can also be used to study weak corrections for bottom quark pair production. This topic will be discussed in a subsequent publication. For a massless bottom-quark, the W, ϕ contributions and the Z, χ triangles differ by at most 1% from the massive case. Hence the effect of the bottom mass is negligible at hadron level.

4 Conclusion

In this article the complete weak corrections to gluon-induced top-quark pair production are calculated – neg-

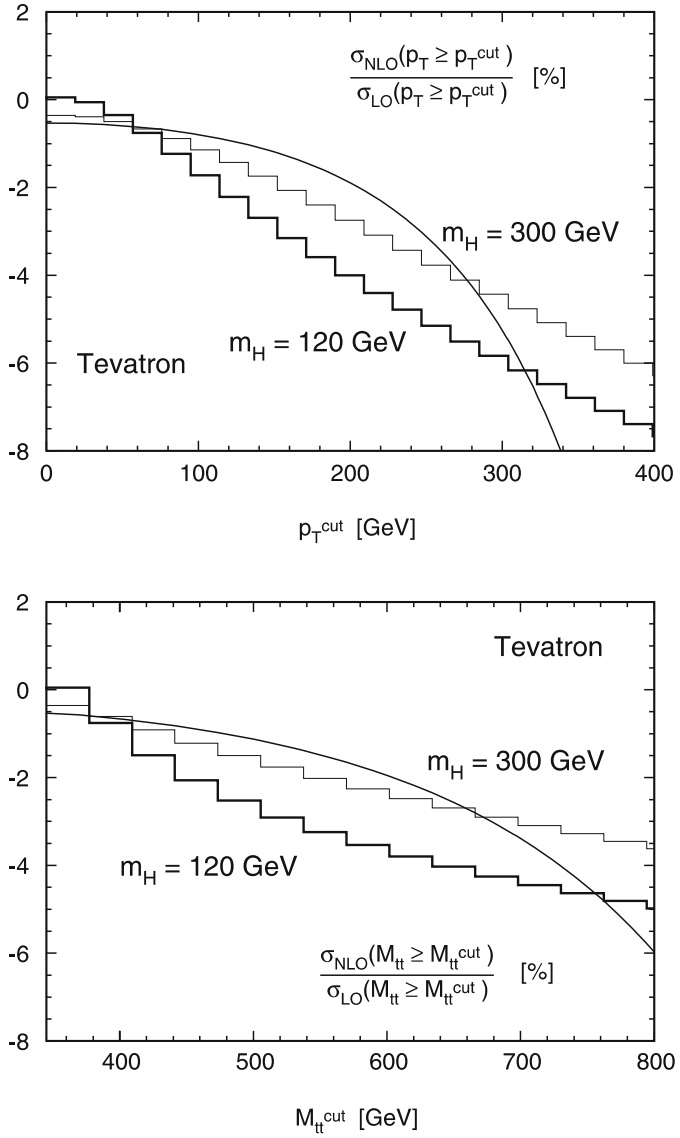

Fig. 15. The relative corrections to the p_{T} and $M_{t\bar{t}}$ distributions, integrated from a lower value in p_{T} and $M_{t\bar{t}}$ to the kinematic limit, for the Tevatron and two Higgs masses ($m_H = 120\,\mathrm{GeV}$ (*bold histogram*), $m_H = 300\,\mathrm{GeV}$ (*thin histogram*)). The *smooth curve* gives an estimate of the corresponding statistical uncertainty for an integrated luminosity of $8\,\mathrm{fb}^{-1}$

lecting purely photonic corrections. In contrast to earlier publications all contributions of one-loop order are taken into account and presented in the form of compact analytic expressions – well suited to be used in experimental analyses. Furthermore, the full dependence on the bottom-quark mass is kept. This allows us to calculate also weak corrections for bottom-quark production using the results presented here. We have shown that the corrections are negligible for the total cross section. For the differential observables, such as the p_{T} distribution or the distribution in the invariant $t\bar{t}$ mass, the corrections can be sizeable. In particular, we find values of up to 15% in kinematic regions that are accessible at the LHC.

Acknowledgements. We would like to thank W. Bernreuther, M. Fücker and Z.-G. Si for useful discussions and for a detailed comparison of results prior to publication.

Appendix A: List of abbreviations

We define as usual

$$
\begin{aligned}
&B_0\big(p_1^2, {m_1}^2, {m_2}^2\big) \\
&= \frac{1}{\mathrm{i}\pi^2}\int \mathrm{d}^d\ell \frac{(2\pi\mu)^{2\varepsilon}}{\big(\ell^2-{m_1}^2+\mathrm{i}\varepsilon\big)\big((\ell+p_1)^2-{m_2}^2+\mathrm{i}\varepsilon\big)}\,, \\
&C_0\big(p_1^2, p_2^2, p_1\cdot p_2, {m_1}^2, {m_2}^2, {m_3}^2\big) \\
&= \frac{1}{\mathrm{i}\pi^2}\int \mathrm{d}^d\ell \frac{(2\pi\mu)^{2\varepsilon}}{\big(\ell^2-{m_1}^2+\mathrm{i}\varepsilon\big)\big((\ell+p_1)^2-{m_2}^2+\mathrm{i}\varepsilon\big)} \\
&\quad\times \frac{1}{\big((\ell+p_1+p_2)^2-{m_3}^2+\mathrm{i}\varepsilon\big)}\,, \\
&D_0\big(p_1^2, p_2^2, p_3^2, p_1\cdot p_2, p_1\cdot p_3, p_2\cdot p_3, {m_1}^2, {m_2}^2, {m_3}^2, {m_4}^2\big) \\
&= \frac{1}{\mathrm{i}\pi^2}\int \mathrm{d}^d\ell \frac{(2\pi\mu)^{2\varepsilon}}{\big(\ell^2-{m_1}^2+\mathrm{i}\varepsilon\big)\big((\ell+p_1)^2-{m_2}^2+\mathrm{i}\varepsilon\big)} \\
&\quad\times \frac{1}{\big((\ell+p_1+p_2)^2-{m_3}^2+\mathrm{i}\varepsilon\big)} \\
&\quad\times \frac{1}{\big((\ell+p_1+p_2+p_3)^2-{m_4}^2+\mathrm{i}\varepsilon\big)}\,.
\end{aligned}
$$

The integrals used in Sect. 2 are

$$
\begin{aligned}
B_0^t &= B_0\big(s, m_t^2, m_t^2\big)\,, \\
B_0^b &= B_0\big(s, m_b^2, m_b^2\big)\,, \\
B_0^Z &= B_0\big(m_t^2, m_t^2, m_Z^2\big)\,, \\
B_0^W &= B_0\big(m_t^2, m_b^2, m_{\mathrm{W}}^2\big)\,, \\
B_0^H &= B_0\big(m_t^2, m_t^2, m_H^2\big)\,, \\
B_0^Z(z) &= B_0\bigg(-\frac{s}{2}(1+\beta z)+m_t^2, m_t^2, m_Z^2\bigg)\,, \\
B_0^W(z) &= B_0\bigg(-\frac{s}{2}(1+\beta z)+m_t^2, m_b^2, m_{\mathrm{W}}^2\bigg)\,, \\
B_0^H(z) &= B_0\bigg(-\frac{s}{2}(1+\beta z)+m_t^2, m_t^2, m_H^2\bigg)\,, \\
C_0^t &= C_0\bigg(0, 0, \frac{s}{2}, m_t^2, m_t^2, m_t^2\bigg)\,, \\
C_0^b &= C_0\bigg(0, 0, \frac{s}{2}, m_b^2, m_b^2, m_b^2\bigg)\,, \\
C_0^Z &= C_0\bigg(s, m_t^2, -\frac{s}{2}, m_t^2, m_t^2, m_Z^2\bigg)\,, \\
C_0^W &= C_0\bigg(s, m_t^2, -\frac{s}{2}, m_b^2, m_b^2, m_{\mathrm{W}}^2\bigg)\,, \\
C_0^H &= C_0\bigg(s, m_t^2, -\frac{s}{2}, m_t^2, m_t^2, m_H^2\bigg)\,, \\
C_0^Z(z) &= C_0\bigg(0, m_t^2, -\frac{s}{4}(1+\beta z), m_t^2, m_t^2, m_Z^2\bigg)\,,
\end{aligned}
$$

$$
\begin{aligned}
C_0^W(z) &= C_0\left(0, m_t^2, -\frac{s}{4}(1+\beta z), m_b^2, m_b^2, m_{\mathrm{W}}^2\right),\\
C_0^H(z) &= C_0\left(0, m_t^2, -\frac{s}{4}(1+\beta z), m_t^2, m_t^2, m_H^2\right),\\
D_0^Z(z) &= D_0\Bigg(0, 0, m_t^2, \frac{s}{2}, -\frac{s}{4}(1-\beta z), -\frac{s}{4}(1+\beta z),\\
&\qquad m_t^2, m_t^2, m_t^2, m_Z^2\Bigg),\\
D_0^W(z) &= D_0\Bigg(0, 0, m_t^2, \frac{s}{2}, -\frac{s}{4}(1-\beta z), -\frac{s}{4}(1+\beta z),\\
&\qquad m_b^2, m_b^2, m_b^2, m_{\mathrm{W}}^2\Bigg),\\
D_0^H(z) &= D_0\Bigg(0, 0, m_t^2, \frac{s}{2}, -\frac{s}{4}(1-\beta z), -\frac{s}{4}(1+\beta z),\\
&\qquad m_t^2, m_t^2, m_t^2, m_H^2\Bigg).
\end{aligned}
\tag{A.1}
$$

The scalar one-loop integrals can be evaluated using for example the library FF [31, 32].

Appendix B: Analytical results

The corrections not yet listed in Sect. 2 are divided in self-energy (Fig. 3b), vertex (Fig. 3a) and box (Fig. 3c) corrections. Self-energy corrections:

$$
\begin{aligned}
\frac{\mathrm{d}\sigma_Z^\Sigma}{\mathrm{d}z} &= \frac{\alpha}{8\pi}\sigma_0\frac{2-N^2(1-\beta z)}{N(1-\beta^2z^2)}\\
&\times\Bigg\{16\big(g_{\mathrm{v}}^{t\,2}+g_{\mathrm{a}}^{t\,2}\big)\frac{1+\beta^2(1-\beta^2)(1-3z^2)-\beta^4z^4}{s(1-\beta^2)(1+\beta^2+2\beta z)}\\
&\times\big(\overline{A}_0\big(m_Z^2\big)-\overline{A}_0\big(m_t^2\big)\big)\\
&+\frac{4}{(1+\beta z)^2(1+\beta^2+2\beta z)}\\
&\times\Bigg[2\big(g_{\mathrm{v}}^{t\,2}+g_{\mathrm{a}}^{t\,2}\big)\frac{m_Z^2}{s}(1-z^2)\beta^2\\
&\times(2+\beta^2-2\beta^4+(3\beta-2\beta^3)z+\beta^4z^2+\beta^3z^3)\\
&+g_{\mathrm{v}}^{t\,2}(2+2\beta^2-4\beta^4-\beta^6+2\beta^8\\
&+(4+2\beta^2-8\beta^4+4\beta^6)\beta z\\
&+(-4+7\beta^2+\beta^4-3\beta^6)\beta^2z^2\\
&-(10-16\beta^2+6\beta^4)\beta^3z^3\\
&+(-5+3\beta^2+\beta^4)\beta^4z^4-(4-2\beta^2)\beta^5z^5-\beta^6z^6)\\
&-g_{\mathrm{a}}^{t\,2}(2+2\beta^2-8\beta^4-3\beta^6+6\beta^8\\
&+2(2-\beta^2-8\beta^4+6\beta^6)\beta z\\
&-(4-5\beta^2-7\beta^4+9\beta^6)\beta^2z^2\\
&-6(1-4\beta^2+3\beta^4)\beta^3z^3\\
&+(1-3\beta^2+3\beta^4)\beta^4z^4\\
&-(4-6\beta^2)\beta^5z^5+\beta^6z^6)\Bigg]\overline{B}_0^Z(z)\\
&-\frac{4}{(1+\beta z)^2}\Bigg[\frac{2}{1-\beta^2}\big(g_{\mathrm{v}}^{t\,2}+g_{\mathrm{a}}^{t\,2}\big)\frac{m_Z^2}{s}\\
&\times(2+2\beta^2-5\beta^4+2\beta^6+(3-2\beta^2)\beta^3z\\
&-3(2-3\beta^2+\beta^4)\beta^2z^2\\
&-3(1-\beta^2)\beta^3z^3-(2-\beta^2)\beta^4z^4-z^5\beta^5)\\
&+\big(g_{\mathrm{v}}^{t\,2}-3g_{\mathrm{a}}^{t\,2}\big)(1-\beta^2)\\
&\times(1+\beta^2-2\beta^4-(2-3\beta^2)\beta^2z^2-\beta^4z^4)\Bigg]\overline{B}_0^Z\\
&+\frac{2}{1+\beta z}\\
&\times\big[\big(2\big(g_{\mathrm{v}}^{t\,2}+g_{\mathrm{a}}^{t\,2}\big)m_Z^2+s(1-\beta^2)\big(g_{\mathrm{v}}^{t\,2}-3g_{\mathrm{a}}^{t\,2}\big)\big)\\
&\times(1+(1-\beta^2)(2\beta^2-\beta z-3\beta^2z^2)-\beta^4z^4)\big]\\
&\times\frac{\mathrm{d}}{\mathrm{d}p^2}B_0^Z\Big|_{p^2=mt^2}\Bigg\}+(z\to-z)\,,
\end{aligned}
\tag{B.1}
$$

$$
\begin{aligned}
\frac{\mathrm{d}\sigma_W^\Sigma}{\mathrm{d}z} &= \frac{\alpha}{\pi}\sigma_0g_{\mathrm{W}}^2\frac{2-N^2(1-\beta z)}{N(1-\beta^2z^2)}\\
&\times\Bigg\{4\frac{1+\beta^2(1-\beta^2)(1-3z^2)-\beta^4z^4}{s(1-\beta^2)(1+\beta^2+2\beta z)}\\
&\times\big(\overline{A}_0\big(m_{\mathrm{W}}^2\big)-\overline{A}_0\big(m_b^2\big)\big)\\
&+\frac{\beta^2(1-z^2)}{2s(1+\beta^2+2\beta z)(1+\beta z)^2}\\
&\times(2+\beta^2-2\beta^4+(3-2\beta^2)\beta z+(z+\beta)\beta^3z^2)\\
&\times\big(s(1+\beta^2+2\beta z)+4\big(m_{\mathrm{W}}^2-m_b^2\big)\big)\overline{B}_0^W(z)\\
&+\frac{1}{2s(1+\beta z)^2}\big[-s\beta^2(1-z^2)\\
&\times(2+\beta^2-2\beta^4+(3-2\beta^2)\beta z+(z+\beta)\beta^3z^2)\\
&-\frac{4}{1-\beta^2}(-2-2\beta^2+5\beta^4-2\beta^6-(3-2\beta^2)\beta^3z\\
&+3(2-3\beta^2+\beta^4)\beta^2z^2+3(1-\beta^2)\beta^3z^3\\
&+(2-\beta^2)\beta^4z^4+z^5\beta^5)\\
&\times\big(m_b^2-m_{\mathrm{W}}^2\big)\big]\overline{B}_0^W\\
&+\frac{1}{4(1+\beta z)}(1+\beta(1-\beta^2)(2\beta-z-3\beta z^2)-\beta^4z^4)\\
&\times\big(s\beta^2-4m_b^2+4m_{\mathrm{W}}^2-s\big)\,\frac{\mathrm{d}}{\mathrm{d}p^2}B_0^W\Big|_{p^2=mt^2}\Bigg\}\\
&+(z\to-z)\,,
\end{aligned}
\tag{B.2}
$$

$$
\begin{aligned}
\frac{\mathrm{d}\sigma_\chi^\Sigma}{\mathrm{d}z} &= 2\frac{\alpha}{\pi}\sigma_0\frac{g_{\mathrm{a}}^{t\,2}}{m_Z^2}\frac{2-N^2(1-\beta z)}{N(1-\beta^2z^2)}\\
&\times\Bigg\{\frac{1+(1-\beta^2)(\beta^2-3\beta^2z^2)-\beta^4z^4}{2(1+\beta^2+2\beta z)}\\
&\times\big(\overline{A}_0\big(m_Z^2\big)-\overline{A}_0\big(m_t^2\big)\big)\\
&+\frac{1-\beta^2}{8(1+\beta^2+2\beta z)}\Bigg[2m_Z^2\frac{\beta^2(1-z^2)}{(1+\beta z)^2}\\
&\times(2+\beta^2-2\beta^4+(3-2\beta^2)\beta z+(z+\beta)\beta^3z^2)\\
&+s(1+\beta^2-\beta^4-3(1-\beta^2)\beta^2z^2-\beta^4z^4)\Bigg]\overline{B}_0^Z(z)\\
&-\frac{m_Z^2}{4(1+\beta z)^2}(2+2\beta^2-5\beta^4+2\beta^6+(3-2\beta^2)\beta^3z
\end{aligned}
$$

$$
\begin{aligned}
&- 3(2-3\beta^2+\beta^4)\beta^2 z^2 - 3(1-\beta^2)\beta^3 z^3 \\
&- (2-\beta^2)\beta^4 z^4 - \beta^5 z^5)\overline{B}_0^Z \\
&+ \frac{m_Z^2 s(1-\beta^2)}{8(1+\beta z)} \\
&\times (1+\beta(1-\beta^2)(2\beta - z - 3\beta z^2) - \beta^4 z^4) \\
&\times \frac{\mathrm{d}}{\mathrm{d}p^2} B_0^Z \Big|_{p^2=mt^2} \Big\} + (z \to -z)\,, \qquad \text{(B.3)}
\end{aligned}
$$

$$
\begin{aligned}
\frac{\mathrm{d}\sigma_\phi^\Sigma}{\mathrm{d}z} &= \frac{\alpha}{\pi}\sigma_0 \frac{g_\mathrm{W}^2}{m_\mathrm{W}^2} \frac{2-N^2(1-\beta z)}{N(1-\beta^2 z^2)} \\
&\times \Bigg\{ \frac{(1+\beta^2(1-\beta^2)(1-3z^2)-\beta^4 z^4)\big(s(1-\beta^2)+4m_b^2\big)}{2s(1-\beta^2)(1+\beta^2+2\beta z)} \\
&\times \big(\overline{A}_0\big(m_\mathrm{W}^2\big) - \overline{A}_0\big(m_b^2\big)\big) \\
&+ \frac{1}{16s(1+\beta z)^2(1+\beta^2+2\beta z)} \\
&\times \big[-\beta^2(1-z^2) \\
&\times (2+\beta^2-2\beta^4+(3-2\beta^2)\beta z+(z+\beta)\beta^3 z^2) \\
&\times \big(16m_b^2\big(m_b^2-m_\mathrm{W}^2\big) - s^2(1-\beta^4+2(1-\beta^2)\beta z) \\
&- 4sm_\mathrm{W}^2(1-\beta^2)\big) \\
&- 8m_b^2 s(-2-2\beta^2+4\beta^4+\beta^6-2\beta^8 \\
&- 2(2+\beta^2-4\beta^4+2\beta^6)\beta z \\
&+ (4-7\beta^2-\beta^4+3\beta^6)\beta^2 z^2 \\
&+ 2(5-8\beta^2+3\beta^4)\beta^3 z^3 + (5-3\beta^2-\beta^4)\beta^4 z^4 \\
&+ 2(2-\beta^2)\beta^5 z^5 + \beta^6 z^6)\big]\overline{B}_0^W(z) \\
&- \frac{1}{16s(1-\beta^2)(1+\beta z)^2}\big[\beta^2 s^2(1-\beta^2)^2(1-z^2) \\
&\times (2+\beta^2-2\beta^4+(3-2\beta^2)\beta z+(z+\beta)\beta^3 z^2) \\
&- 4(-2-2\beta^2+5\beta^4-2\beta^6-(3-2\beta^2)\beta^3 z \\
&+ 3(2-3\beta^2+\beta^4)\beta^2 z^2 \\
&+ 3(1-\beta^2)\beta^3 z^3 + (2-\beta^2)\beta^4 z^4 + \beta^5 z^5) \\
&\times \big(sm_\mathrm{W}^2(1-\beta^2) + 4m_b^2\big(m_\mathrm{W}^2 - m_b^2\big)\big) \\
&+ 8m_b^2 s(1-\beta^2)^2 \\
&\times (1+\beta^2-2\beta^4-(2-3\beta^2)\beta^2 z^2 - \beta^4 z^4)\big]\overline{B}_0^W \\
&- \frac{1}{32(1+\beta z)}(1+\beta(1-\beta^2)(2\beta - z - 3\beta z^2) - \beta^4 z^4) \\
&\times \big(s^2(1-\beta^2)^2 - 4s(1-\beta^2)\big(2m_b^2 + m_\mathrm{W}^2\big) \\
&+ 16m_b^2\big(m_b^2 - m_\mathrm{W}^2\big)\big)\ \frac{\mathrm{d}}{\mathrm{d}p^2} B_0^W \Big|_{p^2=mt^2} \Bigg\} \\
&+ (z \to -z)\,, \qquad \text{(B.4)}
\end{aligned}
$$

$$
\begin{aligned}
\frac{\mathrm{d}\sigma_H^\Sigma}{\mathrm{d}z} &= \frac{\alpha}{\pi}\sigma_0 \frac{g_\mathrm{W}^2}{m_\mathrm{W}^2} \frac{2-N^2(1-\beta z)}{N(1-\beta^2 z^2)} \\
&\times \Bigg\{ \frac{1+\beta^2(1-\beta^2)(1-3z^2)-\beta^4 z^4}{2(1+\beta^2+2\beta z)} \\
&\times \big(\overline{A}_0\big(m_H^2\big) - \overline{A}_0\big(m_t^2\big)\big) \\
&- \frac{(1-\beta^2)}{8(1+2\beta z+\beta^2)(1+\beta z)^2} \\
&\times \big[-2m_H^2\beta^2(1-z^2) \\
&\times (2+\beta^2-2\beta^4+(3-2\beta^2)\beta z+(z+\beta)\beta^3 z^2) \\
&+ s(1+\beta^2-5\beta^4-2\beta^6+4\beta^8 \\
&+ 2(1-\beta^2-5\beta^4+4\beta^6)\beta z \\
&- (2-2\beta^2-5\beta^4+6\beta^6)\beta^2 z^2 \\
&- 2(1-7\beta^2+6\beta^4)\beta^3 z^3 + (2-3\beta^2+2\beta^4)\beta^4 z^4 \\
&- 2(1-2\beta^2)\beta^5 z^5 + \beta^6 z^6)\big]\overline{B}_0^H(z) \\
&+ \frac{1}{4(1+\beta z)^2}\big[s(1-\beta^2)^2 \\
&\times (1+\beta^2-2\beta^4-(2-3\beta^2)\beta^2 z^2 - \beta^4 z^4) \\
&+ m_H^2(-2-2\beta^2+5\beta^4-2\beta^6-(3-2\beta^2)\beta^3 z \\
&+ 3(2-3\beta^2+\beta^4)\beta^2 z^2 \\
&+ 3(1-\beta^2)\beta^3 z^3 + (2-\beta^2)\beta^4 z^4 + \beta^5 z^5)\big]\overline{B}_0^H \\
&- \frac{s(s(1-\beta^2)-m_H^2)(1-\beta^2)}{8(1+\beta z)} \\
&\times (1+\beta(1-\beta^2)(2\beta - z - 3\beta z^2) - \beta^4 z^4) \\
&\times \frac{\mathrm{d}}{\mathrm{d}p^2} B_0^H \Big|_{p^2=mt^2} \Bigg\} + (z \to -z)\,. \qquad \text{(B.5)}
\end{aligned}
$$

Vertex corrections:

$$
\begin{aligned}
\frac{\mathrm{d}\sigma_Z^\mathrm{V}}{\mathrm{d}z} &= \frac{\alpha}{8\pi}\sigma_0 \frac{2-N^2(1-\beta z)}{N(1+\beta z)^2} \Bigg\{ 4(1-\beta^2)\big(g_\mathrm{v}^{t\,2} + g_\mathrm{a}^{t\,2}\big) \\
&+ \frac{16\big(g_\mathrm{v}^{t\,2} + g_\mathrm{a}^{t\,2}\big)}{s(1-\beta z)(1-\beta^2)(1+2\beta z+\beta^2)} \\
&\times (1+2\beta^2-\beta^4+(1+4\beta^2-3\beta^4)\beta z \\
&- 2(1-\beta^2)(2\beta^2 z^2 + 3\beta^3 z^3) \\
&- 2(1+\beta z)\beta^4 z^4)\big(\overline{A}_0\big(m_t^2\big) - \overline{A}_0\big(m_Z^2\big)\big) \\
&+ \frac{4}{(1-\beta^2 z^2)(1+2\beta z+\beta^2)}\Bigg[2\big(g_\mathrm{v}^{t\,2} + g_\mathrm{a}^{t\,2}\big)\frac{m_Z^2}{s} \\
&\times (1-4\beta^2-3\beta^4+4\beta^6+(1-8\beta^2+5\beta^4)\beta z \\
&+ 2(1+2\beta^2-3\beta^4)\beta^2 z^2 + 6(1-\beta^2)\beta^3 z^3 \\
&+ 2\beta^6 z^4 + 2\beta^5 z^5) \\
&- g_\mathrm{v}^{t\,2}(2+3\beta^2-6\beta^4-\beta^6+4\beta^8 \\
&+ (3+7\beta^2-13\beta^4+7\beta^6)\beta z \\
&- (7-18\beta^2+3\beta^4+6\beta^6)\beta^2 z^2 \\
&- (14-26\beta^2+12\beta^4)\beta^3 z^3 \\
&- (10-6\beta^2-2\beta^4)\beta^4 z^4 - (8-4\beta^2)\beta^5 z^5 - 2\beta^6 z^6) \\
&+ g_\mathrm{a}^{t\,2}(-2+5\beta^2-10\beta^4-7\beta^6+12\beta^8 \\
&- (3-9\beta^2+35\beta^4-25\beta^6)\beta z \\
&- (1-6\beta^2-11\beta^4+18\beta^6)\beta^2 z^2 \\
&- 2(1-19\beta^2+18\beta^4)\beta^3 z^3 + 2(1-3\beta^2+3\beta^4)\beta^4 z^4 \\
&- 4(2-3\beta^2)\beta^5 z^5 + 2\beta^6 z^6)\Bigg]\overline{B}_0^Z(z) \\
&+ \frac{4}{(1-\beta^2 z^2)(1-\beta^2)}\Bigg[2\big(g_\mathrm{v}^{t\,2} + g_\mathrm{a}^{t\,2}\big)\frac{m_Z^2}{s} \\
&\times (1+8\beta^2-11\beta^4+4\beta^6+(1+4\beta^2-3\beta^4)\beta z
\end{aligned}
$$

$$
\begin{aligned}
&-2(5-8\beta^2+3\beta^4)\beta^2z^2-6(1-\beta^2)\beta^3z^3\\
&-2(2-\beta^2)\beta^4z^4-2\beta^5z^5)\\
&+(1-\beta^2)^2\big(g_{\rm v}^{t\,2}(1+\beta^2-4\beta^4-(1-\beta^2)\beta z\\
&-2(1-3\beta^2)\beta^2z^2-2\beta^4z^4)\\
&+g_{\rm a}^{t\,2}(1-7\beta^2+12\beta^4-(1-\beta^2)\beta z\\
&+6(1-3\beta^2)\beta^2z^2+6\beta^4z^4)\big)\Big]\overline{B}_0^Z\\
&+2\big(g_{\rm v}^{t\,2}+g_{\rm a}^{t\,2}\big)s(1-\beta^2)^2C_0^Z(z)\\
&-\frac{4}{1-\beta z}\\
&\times\big(\big(\big(g_{\rm v}^{t\,2}-3g_{\rm a}^{t\,2}\big)s(1-\beta^2)+2\big(g_{\rm v}^{t\,2}+g_{\rm a}^{t\,2}\big)m_Z^2\big)\\
&\times(1+\beta(1-\beta^2)(2\beta-z-3\beta z^2)-\beta^4z^4)\big)\\
&\times\frac{\mathrm{d}}{\mathrm{d}p^2}B_0^Z\Big|_{p^2=mt^2}\Big\}+(z\to-z)\,, \qquad \text{(B.6)}
\end{aligned}
$$

$$
\begin{aligned}
\frac{\mathrm{d}\sigma_W^{\rm V}}{\mathrm{d}z}=&\frac{\alpha}{\pi}\sigma_0g_{\rm W}^2\frac{2-N^2(1-\beta z)}{N(1+\beta z)^2}\Big\{(1-\beta^2)\\
&+\frac{4}{s(1-\beta z)(1-\beta^2)(1+2\beta z+\beta^2)}\\
&\times(1+2\beta^2-\beta^4+(1+4\beta^2-3\beta^4)\beta z\\
&-2(1-\beta^2)(2\beta^2z^2+3\beta^3z^3)-2(1+\beta z)\beta^4z^4)\\
&\times\big(\overline{A}_0\big(m_b^2\big)-\overline{A}_0\big(m_{\rm W}^2\big)\big)\\
&+\frac{1}{2s(1-\beta^2z^2)(1+2\beta z+\beta^2)}\\
&\times\big[4\big(m_{\rm W}^2-m_b^2\big)\big(1-4\beta^2-3\beta^4+4\beta^6\\
&+(1-8\beta^2+5\beta^4)\beta z+2(1+2\beta^2-3\beta^4)\beta^2z^2\\
&+6(1-\beta^2)\beta^3z^3+2\beta^6z^4+2\beta^5z^5\big)\\
&-s(1+2\beta z+\beta^2)\\
&\times(3+3\beta^4-4\beta^6-(1-8\beta^2+5\beta^4)\beta z\\
&-6(1-\beta^4)\beta^2z^2-6(1-\beta^2)\beta^3z^3\\
&-2\beta^6z^4-2\beta^5z^5)\big]\overline{B}_0^W(z)\\
&+\frac{1}{2s(1-\beta^2)(1-\beta^2z^2)}\big[4\big(m_{\rm W}^2-m_b^2\big)\\
&\times(1+8\beta^2-11\beta^4+4\beta^6+(1+4\beta^2-3\beta^4)\beta z\\
&-2(5-8\beta^2+3\beta^4)\beta^2z^2-6(1-\beta^2)\beta^3z^3\\
&-2(2-\beta^2)\beta^4z^4-2\beta^5z^5)\\
&+s(1-\beta^2)(3+3\beta^4-4\beta^6-(1-8\beta^2+5\beta^4)\beta z\\
&-6(1-\beta^4)\beta^2z^2-6(1-\beta^2)\beta^3z^3\\
&-2\beta^6z^4-2\beta^5z^5)\big]\overline{B}_0^W\\
&+2m_b^2(1-\beta^2)C_0^W(z)\\
&+\frac{s(1-\beta^2)+4(m_b^2-m_{\rm W}^2)}{2(1-\beta z)}\\
&\times(1+\beta(1-\beta^2)(2\beta-z-3\beta z^2)-\beta^4z^4)\\
&\frac{\mathrm{d}}{\mathrm{d}p^2}B_0^W\Big|_{p^2=mt^2}\Big\}+(z\to-z)\,, \qquad \text{(B.7)}
\end{aligned}
$$

$$
\begin{aligned}
\frac{\mathrm{d}\sigma_\chi^{\rm V}}{\mathrm{d}z}=&2\frac{\alpha}{\pi}\sigma_0\frac{g_{\rm a}^{t\,2}}{m_Z^2}\frac{2-N^2(1-\beta z)}{N(1+\beta z)^2}\\
&\times\Big\{\frac{s(1-\beta^2)^2}{8}+\frac{1}{2(1-\beta z)(1+2\beta z+\beta^2)}\\
&\times(1+2\beta^2-\beta^4+(1+4\beta^2-3\beta^4)\beta z\\
&-2(1-\beta^2)(2\beta^2z^2+3\beta^3z^3)\\
&-2(1+\beta z)\beta^4z^4)\big(\overline{A}_0\big(m_t^2\big)-\overline{A}_0\big(m_Z^2\big)\big)\\
&+\frac{(1-\beta^2)}{8(1-\beta^2z^2)(1+2\beta z+\beta^2)}\\
&\times\big[2m_Z^2(1-4\beta^2-3\beta^4+4\beta^6\\
&+(1-8\beta^2+5\beta^4)\beta z+2(1+2\beta^2-3\beta^4)\beta^2z^2\\
&+6(1-\beta^2)\beta^3z^3+2\beta^6z^4+2\beta^5z^5)\\
&+s\beta(-(1+\beta^4)\beta+(1-7\beta^2+\beta^4+\beta^6)z\\
&+(3-12\beta^2+7\beta^4)\beta z^2+6(1-\beta^2)\beta^2z^3\\
&+2(4-3\beta^2)\beta^3z^4+4\beta^4z^5+2\beta^5z^6)\big]\overline{B}_0^Z(z)\\
&+\frac{1}{8(1-\beta^2z^2)}\big[2m_Z^2(1+8\beta^2-11\beta^4+4\beta^6\\
&+(1+4\beta^2-3\beta^4)\beta z-2(5-8\beta^2+3\beta^4)\beta^2z^2\\
&-6(1-\beta^2)\beta^3z^3-2(2-\beta^2)\beta^4z^4-2\beta^5z^5)\\
&-s(1-\beta^2)^2(1+2\beta z+\beta^2)(1-\beta z)\big]\overline{B}_0^Z\\
&-\frac{s^2(1-\beta^2)^2(1+2\beta z+\beta^2)}{16}C_0^Z(z)\\
&-\frac{m_Z^2s(1-\beta^2)}{4(1-\beta z)}\\
&\times(1+\beta(1-\beta^2)(2\beta-z-3\beta z^2)-\beta^4z^4)\\
&\times\frac{\mathrm{d}}{\mathrm{d}p^2}B_0^Z\Big|_{p^2=mt^2}\Big\}+(z\to-z)\,, \qquad \text{(B.8)}
\end{aligned}
$$

$$
\begin{aligned}
\frac{\mathrm{d}\sigma_\phi^{\rm V}}{\mathrm{d}z}=&\frac{\alpha}{\pi}\sigma_0\frac{2-N^2(1-\beta z)}{N(1+\beta z)^2}\frac{g_{\rm W}^2}{m_{\rm W}^2}\\
&\times\Big\{\frac{(1-\beta^2)\big(s(1-\beta^2)+4m_b^2\big)}{8}\\
&+\frac{s(1-\beta^2)+4m_b^2}{2s(1-\beta z)(1+2\beta z+\beta^2)(1-\beta^2)}\\
&\times(1+2\beta^2-\beta^4+(1+4\beta^2-3\beta^4)\beta z\\
&-2(1-\beta^2)(2\beta^2z^2+3\beta^3z^3)-2(1+\beta z)\beta^4z^4)\\
&\times\big(\overline{A}_0\big(m_b^2\big)-\overline{A}_0\big(m_{\rm W}^2\big)\big)\\
&+\frac{1}{16s(1-\beta^2z^2)(1+2\beta z+\beta^2)}\\
&\times\big[\big(4m_{\rm W}^2\big(s(1-\beta^2)+4m_b^2\big)-16m_b^4\big)\\
&\times(1-4\beta^2-3\beta^4+4\beta^6+(1-8\beta^2+5\beta^4)\beta z\\
&+2(1+2\beta^2-3\beta^4)\beta^2z^2+6(1-\beta^2)\beta^3z^3\\
&+2\beta^6z^4+2\beta^5z^5)\\
&+8\beta m_b^2s(-(3-4\beta^2-\beta^4+4\beta^6)\beta\\
&+(1-11\beta^2+13\beta^4-7\beta^6)z\\
&+(5-18\beta^2+5\beta^4+6\beta^6)\beta z^2\\
&+2(5-11\beta^2+6\beta^4)\beta^2z^3+2(5-3\beta^2-\beta^4)\beta^3z^4
\end{aligned}
$$

$$
\begin{aligned}
&+4(2-\beta^2)\beta^4z^5+2\beta^5z^6)\\
&+s^2(1-\beta^2)(1+2\beta z+\beta^2)\\
&\times(1-4\beta^2-3\beta^4+4\beta^6+(1-8\beta^2+5\beta^4)\beta z\\
&+2(1+2\beta^2-3\beta^4)\beta^2z^2+6(1-\beta^2)\beta^3z^3\\
&+2\beta^6z^4+2\beta^5z^5)\big]\overline{B}_0^W(z)\\
&+\frac{1}{16s(1-\beta^2)(1-\beta^2z^2)}\\
&\times\big[\big(4m_{\mathrm{W}}^2\big(s(1-\beta^2)+4m_b^2\big)-16m_b^4\big)\\
&\times(1+8\beta^2-11\beta^4+4\beta^6+(1+4\beta^2-3\beta^4)\beta z\\
&-2(5-8\beta^2+3\beta^4)\beta^2z^2-6(1-\beta^2)\beta^3z^3\\
&-2(2-\beta^2)\beta^4z^4-2\beta^5z^5)\\
&-8m_b^2s(1-\beta^2)^2(1-\beta^2+4\beta^4+(1-\beta^2)\beta z\\
&-6\beta^4z^2+2\beta^4z^4)\\
&-s^2(1-\beta^2)^2(1-4\beta^2-3\beta^4+4\beta^6\\
&+(1-8\beta^2+5\beta^4)\beta z+2(1+2\beta^2-3\beta^4)\beta^2z^2\\
&+6(1-\beta^2)\beta^3z^3+2\beta^6z^4+2\beta^5z^5)\big]\overline{B}_0^W\\
&-\frac{1}{4}m_b^2(1-\beta^2)\big(s\beta^2+4s\beta z+3s-4m_b^2\big)C_0^W(z)\\
&+\frac{1}{16(1-\beta z)}\big(s^2(1-\beta^2)^2\\
&-4s\big(m_{\mathrm{W}}^2+2m_b^2\big)(1-\beta^2)+16m_b^2\big(m_b^2-m_{\mathrm{W}}^2\big)\big)\\
&\times(1+\beta(1-\beta^2)(2\beta-z-3\beta z^2)-\beta^4z^4)\\
&\times\frac{\mathrm{d}}{\mathrm{d}p^2}B_0^W\bigg|_{p^2=mt^2}\bigg\}+(z\to-z)\,, \qquad \text{(B.9)}
\end{aligned}
$$

$$
\begin{aligned}
\frac{\mathrm{d}\sigma_H^{\mathrm{V}}}{\mathrm{d}z}=\frac{\alpha}{\pi}\sigma_0\frac{g_{\mathrm{W}}^2}{m_{\mathrm{W}}^2}\frac{2-N^2(1-\beta z)}{N(1+\beta z)^2}\bigg\{&\frac{s(1-\beta^2)^2}{8}\\
&+\frac{1}{2(1-\beta z)(1+2\beta z+\beta^2)}\\
&\times(1+2\beta^2-\beta^4+(1+4\beta^2-3\beta^4)\beta z\\
&-2(1-\beta^2)(2\beta^2z^2+3\beta^3z^3)-2(1+\beta z)\beta^4z^4)\\
&\times\big(\overline{A}_0\big(m_t^2\big)-\overline{A}_0\big(m_H^2\big)\big)\\
&+\frac{1-\beta^2}{8(1-\beta^2z^2)(1+2\beta z+\beta^2)}\\
&\times\big[2m_H^2(1-4\beta^2-3\beta^4+4\beta^6+(1-8\beta^2+5\beta^4)\beta z\\
&+2(1+2\beta^2-3\beta^4)\beta^2z^2\\
&+6(1-\beta^2)\beta^3z^3+2\beta^6z^4+2\beta^5z^5)\\
&+s\beta((3-8\beta^2-5\beta^4+8\beta^6)\beta\\
&+(1+\beta^2-23\beta^4+17\beta^6)z-(1-11\beta^4+12\beta^6)\beta z^2\\
&-2(1-13\beta^2+12\beta^4)\beta^2z^3+2(2-3\beta^2+2\beta^4)\beta^3z^4\\
&-4(1-2\beta^2)\beta^4z^5+2\beta^5z^6)\big]\overline{B}_0^H(z)\\
&+\frac{1}{8(1-\beta^2z^2)}\big[2m_H^2(1+8\beta^2-11\beta^4+4\beta^6\\
&+(1+4\beta^2-3\beta^4)\beta z-2(5-8\beta^2+3\beta^4)\beta^2z^2\\
&-6(1-\beta^2)\beta^3z^3-2(2-\beta^2)\beta^4z^4-2\beta^5z^5)\\
&-s(1-\beta^2)^2(1+5\beta^2-8\beta^4+(1-\beta^2)\beta z\\
&-6(1-2\beta^2)\beta^2z^2-4\beta^4z^4)\big]\overline{B}_0^H\\
&+\frac{s^2(1-\beta^2)^2(3+2\beta z-\beta^2)}{16}C_0^H(z)\\
&+\frac{s(1-\beta^2)(s(1-\beta^2)-m_H^2)}{4(1-\beta z)}\\
&\times(1+\beta(1-\beta^2)(2\beta-z-3\beta z^2)-\beta^4z^4)\\
&\times\frac{\mathrm{d}}{\mathrm{d}p^2}B_0^H\bigg|_{p^2=mt^2}\bigg\}+(z\to-z)\,. \qquad \text{(B.10)}
\end{aligned}
$$

Box corrections:

$$
\begin{aligned}
\frac{\mathrm{d}\sigma_Z^{\square}}{\mathrm{d}z}=\frac{\alpha}{8\pi}\sigma_0\frac{N^2(1-\beta z)-2}{N(1-\beta^2z^2)}&\\
\times\bigg\{&-2\big(g_{\mathrm{v}}^{t\,2}+g_{\mathrm{a}}^{t\,2}\big)\beta z(1-z^2)\\
&+8\big(g_{\mathrm{v}}^{t\,2}+g_{\mathrm{a}}^{t\,2}\big)\frac{\beta(1-z^2)(4\beta-z-2\beta z^2)}{s(1+\beta^2+2\beta z)}\\
&\times\big(\overline{A}_0\big(m_t^2\big)-\overline{A}_0\big(m_Z^2\big)\big)\\
&-2\bigg[2\big(g_{\mathrm{v}}^{t\,2}+g_{\mathrm{a}}^{t\,2}\big)\frac{m_Z^2}{s\beta}z(5-4\beta^2-(3-2\beta^2)z^2)\\
&-g_{\mathrm{v}}^{t\,2}(2+(1-4\beta^2)\beta z-2z^2+(1+2\beta^2)\beta z^3)\\
&-g_{\mathrm{a}}^{t\,2}(2-3(5-4\beta^2)\beta z-2z^2+3(3-2\beta^2)\beta z^3)\bigg]\overline{B}_0^t\\
&+\frac{4}{1+\beta z}\bigg[-\big(g_{\mathrm{a}}^{t\,2}+g_{\mathrm{v}}^{t\,2}\big)\frac{m_Z^2}{s\beta}(-6\beta^3\\
&-(5-8\beta^2+4\beta^4)z-(5-12\beta^2)\beta z^2\\
&+(3-4\beta^2+2\beta^4)z^3+(3-4\beta^2)\beta z^4)\\
&+g_{\mathrm{v}}^{t\,2}(5\beta^2-3\beta^4+(1+\beta^2-2\beta^4)\beta z\\
&+(1-4\beta^2+3\beta^4)z^2-(1-\beta^2)\beta^3z^3-(1+\beta^2)\beta^2z^4)\\
&-g_{\mathrm{a}}^{t\,2}(3\beta^2-5\beta^4-3(3-5\beta^2+2\beta^4)\beta z\\
&-(1+8\beta^2-9\beta^4)z^2\\
&+(4-7\beta^2+3\beta^4)\beta z^3+(5-3\beta^2)\beta^2z^4)\bigg]\overline{B}_0^Z\\
&+2\bigg[8\big(g_{\mathrm{v}}^{t\,2}+g_{\mathrm{a}}^{t\,2}\big)\frac{m_Z^4}{s}\\
&+4m_Z^2\big(g_{\mathrm{v}}^{t\,2}(3+\beta z)-g_{\mathrm{a}}^{t\,2}(1-4\beta^2-\beta z)\big)\\
&+s\big(g_{\mathrm{v}}^{t\,2}(4+2\beta^2-\beta^4+2(2-\beta^2)\beta z+\beta^2z^2)\\
&+g_{\mathrm{a}}^{t\,2}(4-6\beta^2+7\beta^4-2(2-3\beta^2)\beta z+\beta^2z^2)\big)\bigg]C_0^t\\
&+2\bigg[-2\big(g_{\mathrm{v}}^{t\,2}+g_{\mathrm{a}}^{t\,2}\big)\frac{m_Z^4}{s\beta}z(5-8\beta^2-3z^2+2\beta^2z^2)\\
&+2m_Z^2\big(g_{\mathrm{v}}^{t\,2}(1+\beta^2+4\beta z-(1-\beta^2)z^2+2\beta z^3)\\
&+g_{\mathrm{a}}^{t\,2}(1+\beta^2-4(3-4\beta^2)\beta z-(1-\beta^2)z^2\\
&+2(3-2\beta^2)\beta z^3)\big)\\
&+\beta s\big(g_{\mathrm{v}}^{t\,2}((4-\beta^2)\beta+\beta^4z^3+4(1+\beta^2-\beta^4)z\\
&-\beta^3z^2+\beta^2z^3)\\
&-g_{\mathrm{a}}^{t\,2}(-3\beta^3-4(1-3\beta^2+3\beta^4)z\\
&+(4-3\beta^2)\beta z^2-(5-3\beta^2)\beta^2z^3)\big)\bigg]C_0^Z
\end{aligned}
$$

$$
\begin{aligned}
&+\frac{4}{(1+\beta z)(1+\beta^2+2\beta z)}\\
&\times\Big[2\big(g_{\rm v}^{t\,2}+g_{\rm a}^{t\,2}\big)\frac{m_Z^2}{s}\beta(z+\beta)\\
&\times(1-3\beta^2+(1-2\beta^2)\beta z+2\beta^2z^2+\beta^3z^3)\\
&-g_{\rm v}^{t\,2}(1+8\beta^2-3\beta^6+(4+14\beta^2-11\beta^4-2\beta^6)\beta z\\
&-(2+\beta^2+3\beta^4)\beta^2z^2-(11-6\beta^2-\beta^4)\beta^3z^3\\
&-2(1-\beta^2)\beta^4z^4-\beta^5z^5\big)\\
&-g_{\rm a}^{t\,2}(1+5\beta^6+(4-10\beta^2+5\beta^4+6\beta^6)\beta z\\
&+(2-17\beta^2+9\beta^4)\beta^2z^2+(1-2\beta^2-3\beta^4)\beta^3z^3\\
&+6(1-\beta^2)\beta^4z^4-\beta^5z^5)\Big]\overline{B}_0^Z(z)\\
&-2\Big[8\big(g_{\rm v}^{t\,2}+g_{\rm a}^{t\,2}\big)\frac{m_Z^4}{s}(1+\beta z)\\
&+4m_Z^2(1+\beta z)\\
&\times\big(3g_{\rm v}^{t\,2}-g_{\rm a}^{t\,2}+4\beta^2g_{\rm a}^{t\,2}+\big(g_{\rm v}^{t\,2}+g_{\rm a}^{t\,2}\big)\beta z\big)\\
&+s\big(g_{\rm v}^{t\,2}(4+2\beta^2-\beta^4+(7+2\beta^2-2\beta^4)\beta z\\
&+(5-2\beta^2)\beta^2z^2+\beta^3z^3)\\
&+g_{\rm a}^{t\,2}(4-6\beta^2+7\beta^4-(1-2\beta^2-6\beta^4)\beta z\\
&-3(1-2\beta^2)\beta^2z^2+\beta^3z^3)\big)\Big]C_0^Z(z)\\
&+\Big[16\big(g_{\rm v}^{t\,2}+g_{\rm a}^{t\,2}\big)\frac{m_Z^6}{s}+8m_Z^4\big(g_{\rm v}^{t\,2}(3+\beta^2+2\beta z)\\
&-g_{\rm a}^{t\,2}(1-5\beta^2-2\beta z)\big)\\
&+2sm_Z^2\big(g_{\rm v}^{t\,2}(4+9\beta^2-2\beta^4+10\beta z+(2+\beta^2)\beta^2z^2)\\
&+g_{\rm a}^{t\,2}(4-7\beta^2+14\beta^4-2(3-8\beta^2)\beta z\\
&+(2+\beta^2)\beta^2z^2)\big)\\
&+s^2\big(g_{\rm v}^{t\,2}(1+7\beta^2-\beta^4-2\beta^6+(3+8\beta^2-4\beta^4)\beta z\\
&+(1+3\beta^2-\beta^4)\beta^2z^2+\beta^3z^3)\\
&-g_{\rm a}^{t\,2}(3-7\beta^2+5\beta^4-6\beta^6-(3-8\beta^2+12\beta^4)\beta z\\
&+3(1-\beta^2-\beta^4)\beta^2z^2-\beta^3z^3)\big)\Big]D_0^Z(z)\Big\}\\
&+(z\to-z)\,,
\end{aligned}
\tag{B.11}
$$

$$
\begin{aligned}
\frac{{\rm d}\sigma_W^{\square}}{{\rm d}z}=\frac{\alpha}{2\pi}\sigma_0g_{\rm W}^2\frac{N^2(1-\beta z)-2}{N(1-\beta^2z^2)}\Big\{&-(1-z^2)\beta z\\
&+\frac{4\beta(1-z^2)(4\beta-z-2\beta z^2)}{s(1+\beta^2+2\beta z)}\big(\overline{A}_0\big(m_b^2\big)-\overline{A}_0\big(m_{\rm W}^2\big)\big)\\
&-\frac{1}{2s\beta}\big[4\big(m_{\rm W}^2-m_b^2\big)z(5-4\beta^2-(3-2\beta^2)z^2)\\
&-s(4\beta-(5+5\beta^2-4\beta^4)z-4\beta z^2\\
&+(3+5\beta^2-2\beta^4)z^3)\big]\overline{B}_0^b\\
&+\frac{1}{2s\beta(1+\beta z)}\big[4\big(m_{\rm W}^2-m_b^2\big)\\
&\times(6\beta^3+(5-8\beta^2+4\beta^4)z+(5-12\beta^2)\beta z^2\\
&-(3-4\beta^2+2\beta^4)z^3-(3-4\beta^2)\beta z^4\big)\\
&+s(2(5-\beta^2)\beta^3+(1-\beta^2)((5+12\beta^2-4\beta^4)z\\
&+9\beta z^2-(3+4\beta^2-2\beta^4)z^3)-\beta(3+5\beta^2)z^4)\big]\overline{B}_0^W\\
&+\frac{1}{2s}\big[\big(4\big(m_{\rm W}^2-m_b^2\big)\big)^2+8m_{\rm W}^2s(2+\beta^2+\beta z)\\
&-8m_b^2s\beta(2\beta+z)\\
&+s^2(7+2\beta^2+\beta^4+2(1+\beta^2)\beta z+2\beta^2z^2)\big]C_0^b\\
&+\frac{1}{8s\beta}\big[-\big(4\big(m_{\rm W}^2-m_b^2\big)\big)^2z(5-8\beta^2-(3-2\beta^2)z^2)\\
&+8m_{\rm W}^2s(2(1+\beta^2)\beta-(5-5\beta^2-8\beta^4)z\\
&-2(1-\beta^2)\beta z^2+(3+3\beta^2-2\beta^4)z^3)\\
&-8m_b^2s(2(1+\beta^2)\beta-(1+\beta^2)(5-8\beta^2)z\\
&-2(1-\beta^2)\beta z^2+(1+\beta^2)(3-2\beta^2)z^3)\\
&-s^2(-4(1+4\beta^2+\beta^4)\beta+(5-30\beta^2+\beta^4-8\beta^6)z\\
&+4(1+2\beta^2-\beta^4)\beta z^2\\
&-(3+4\beta^2+11\beta^4-2\beta^6)z^3)\big]C_0^W\\
&+\frac{1}{s(1+\beta z)(1+\beta^2+2\beta z)}\big[4\big(m_{\rm W}^2-m_b^2\big)\\
&\times\beta(z+\beta)(1-3\beta^2+(1-2\beta^2)\beta z+2\beta^2z^2+\beta^3z^3)\\
&-s(1+\beta^2+2\beta z)(2+5\beta^2-\beta^4\\
&+(3-6\beta^2+2\beta^4)\beta z\\
&-(7-2\beta^2)\beta^2z^2+(2-\beta^2)\beta^3z^3-\beta^4z^4)\big]\overline{B}_0^W(z)\\
&-\frac{1}{2s}\big[\big(4\big(m_{\rm W}^2-m_b^2\big)\big)^2(1+\beta z)\\
&+8m_{\rm W}^2s(1+\beta z)(2+\beta^2+\beta z)\\
&-8m_b^2s\beta(\beta+z)(2+\beta z)\\
&+s^2(1+\beta z)(7+2\beta^2+\beta^4\\
&+2(1+\beta^2)\beta z+2\beta^2z^2)\big]C_0^W(z)\\
&+\frac{1}{8s}\big[\big(4\big(m_{\rm W}^2-m_b^2\big)\big)^3\\
&+8s\big(2\big(m_{\rm W}^2-m_b^2\big)^2(3\beta^2+4\beta z)\\
&+10m_{\rm W}^4+2m_b^4(1+2\beta^2z^2)-4m_{\rm W}^2m_b^2(3+\beta^2z^2)\big)\\
&+4s^2\big(m_{\rm W}^2(11+8\beta^2+3\beta^4\\
&+4(3+2\beta^2)\beta z+6\beta^2z^2)\\
&-m_b^2(11-4\beta^2+3\beta^4+8(1+\beta^2)\beta z\\
&+2(6+\beta^2)\beta^2z^2)\big)\\
&+s^3(1+\beta^2+2\beta z)(7+2\beta^2+\beta^4\\
&+2(1+\beta^2)\beta z+2\beta^2z^2)\big]D_0^W(z)\Big\}\\
&+(z\to-z)\,,
\end{aligned}
\tag{B.12}
$$

$$
\begin{aligned}
\frac{{\rm d}\sigma_\chi^{\square}}{{\rm d}z}=\frac{\alpha}{2\pi}\sigma_0m_t^2\frac{g_{\rm a}^{t\,2}}{m_Z^2}\frac{N^2(1-\beta z)-2}{N(1-\beta^2z^2)}\Big\{&-\beta z(1-z^2)\\
&+\frac{4\beta(1-z^2)(4\beta-z-2\beta z^2)}{s(1+\beta^2+2\beta z)}\big(\overline{A}_0\big(m_t^2\big)-\overline{A}_0\big(m_Z^2\big)\big)\\
&-\frac{1}{s\beta}\big[2m_Z^2z(5-4\beta^2-(3-2\beta^2)z^2)\\
&-s\beta(1-z^2)(2+\beta z)\big]\overline{B}_0^t\\
&+\frac{1}{s\beta(1+\beta z)}\big[2m_Z^2(6\beta^3+(5-8\beta^2+4\beta^4)z
\end{aligned}
$$

$$
\begin{aligned}
&+(5-12\beta^2)\beta z^2\\
&-(3-4\beta^2+2\beta^4)z^3-(3-4\beta^2)\beta z^4)\\
&-2\beta s(1-\beta^2)(2-\beta^2+\beta z-z^2-\beta z^3)\big]\overline{B}_0^Z\\
&+\frac{1}{s}\big[8m_Z^4+4\beta s(\beta+z)m_Z^2\\
&+s^2(2-2\beta^2+\beta^4+2\beta z+\beta^2z^2)\big]C_0^t\\
&-\frac{1}{s\beta}\big[2m_Z^4z(5-8\beta^2-(3-2\beta^2)z^2)\\
&-2m_Z^2s\beta(1+\beta^2-2(1-2\beta^2)\beta z-(1-\beta^2)z^2\\
&+(1-\beta^2)\beta z^3)-s^2\beta^2(\beta+z)(1+\beta z)\big]C_0^Z\\
&+\frac{1}{s(1+\beta z)(1+\beta^2+2\beta z)}\big[4m_Z^2\beta(\beta+z)\\
&\times(1-3\beta^2+(1-2\beta^2)\beta z+2z^2\beta^2+\beta^3z^3)\\
&+2s(1-4\beta^2+\beta^6+(2-10\beta^2+3\beta^4)\beta z\\
&+(3-5\beta^2)\beta^2z^2+2(3-\beta^2)\beta^3z^3\\
&+4\beta^4z^4+\beta^5z^5)\big]\overline{B}_0^Z(z)\\
&-\frac{1}{s}\big[4\big(2m_Z^4+m_Z^2s\beta(\beta+z)\big)(1+\beta z)\\
&+s^2(2-2\beta^2+\beta^4+3\beta z+3\beta^2z^2+\beta^3z^3)\big]C_0^Z(z)\\
&+\frac{1}{2s}\big[16m_Z^6+16m_Z^4s\beta(\beta+z)\\
&+2m_Z^2s^2\\
&\times(2-\beta^2+2\beta^4+2(1+2\beta^2)\beta z+(2+\beta^2)\beta^2z^2)\\
&+s^3\beta(\beta+z)(1+\beta z)^2\big]D_0^Z(z)\Big\}+(z\to-z)\,,
\end{aligned}
\tag{B.13}
$$

$$
\begin{aligned}
\frac{\mathrm{d}\sigma_\phi^\Box}{\mathrm{d}z}&=\frac{\alpha}{4\pi}\sigma_0\frac{g_\mathrm{W}^2}{m_\mathrm{W}^2}\frac{N^2(1-\beta z)-2}{N(1-\beta^2z^2)}\\
&\times\Big\{-\frac{\beta}{4}z(1-z^2)\big(s(1-\beta^2)+4m_b^2\big)\\
&+\frac{\beta(1-z^2)\big(s(1-\beta^2)+4m_b^2\big)(4\beta-z-2\beta z^2)}{s(1+\beta^2+2\beta z)}\\
&\times\big(\overline{A}_0\big(m_b^2\big)-\overline{A}_0\big(m_\mathrm{W}^2\big)\big)\\
&+\frac{1}{8s\beta}\big[\big(16m_b^2\big(m_b^2-m_\mathrm{W}^2\big)\\
&-4m_\mathrm{W}^2s(1-\beta^2)\big)z(5-4\beta^2-(3-2\beta^2)z^2)\\
&+8m_b^2s\beta(2+(5-4\beta^2)\beta z-2z^2-(3-2\beta^2)\beta z^3)\\
&+s^2(1-\beta^2)(4\beta-(5-3\beta^2-4\beta^4)z\\
&-4\beta z^2+(3-3\beta^2-2\beta^4)z^3)\big]\overline{B}_0^b\\
&-\frac{1}{8s\beta(1+\beta z)}\\
&\times\big[\big(16m_b^2\big(m_b^2-m_\mathrm{W}^2\big)-4m_\mathrm{W}^2s(1-\beta^2)\big)\\
&\times(6\beta^3+(5-8\beta^2+4\beta^4)z+(5-12\beta^2)\beta z^2\\
&-(3-4\beta^2+2\beta^4)z^3-(3-4\beta^2)\beta z^4)\\
&+16m_b^2s\beta(1-\beta^2)(2-3\beta^2+(3-2\beta^2)\beta z\\
&-(1-3\beta^2)z^2-(2-\beta^2)\beta z^3-\beta^2z^4)\\
&+s^2(1-\beta^2)^2(8\beta-2\beta^3-(5-4\beta^2-4\beta^4)z\\
&-9\beta z^2+(3-4\beta^2-2\beta^4)z^3+3\beta z^4)\big]\overline{B}_0^W\\
&+\frac{1}{8s}\big[64m_b^6+16m_b^4\big(s(1-\beta^2)-8m_\mathrm{W}^2-2zs\beta\big)\\
&+16m_\mathrm{W}^4\big(s(1-\beta^2)+4m_b^2\big)+32m_b^2m_\mathrm{W}^2s(1+\beta z)\\
&+4s^2m_b^2(3-2\beta^2+\beta^4+4(2-\beta^2)\beta z+2\beta^2z^2)\\
&+8s^2m_\mathrm{W}^2\beta(1-\beta^2)(\beta+z)\\
&+s^3(1-\beta^2)(3-2\beta^2+\beta^4\\
&+2(1+\beta^2)\beta z+2\beta^2z^2)\big]C_0^b\\
&+\frac{1}{32s\beta}\\
&\times\big[-16\big(4m_b^6+m_\mathrm{W}^4\big(s(1-\beta^2)+4m_b^2\big)-8m_b^4m_\mathrm{W}^2\big)\\
&\times z(5-8\beta^2-(3-2\beta^2)z^2)\\
&-16m_b^4s(4(1+\beta^2)\beta-(5-17\beta^2+8\beta^4)z\\
&-4(1-\beta^2)\beta z^2+(3-9\beta^2+2\beta^4)z^3)\\
&+64m_\mathrm{W}^2m_b^2s\beta(1+\beta^2+2\beta z-(1-\beta^2)z^2)\\
&+4s^2m_b^2(8(2-\beta^2)\beta^3+(5-2\beta^2+21\beta^4-8\beta^6)z\\
&+8(2-\beta^2)\beta^3z^2-(3-\beta^4-2\beta^6)z^3)\\
&+8m_\mathrm{W}^2s^2(1-\beta^2)(2(1+\beta^2)\beta-(5-\beta^2-8\beta^4)z\\
&-2(1-\beta^2)\beta z^2+(3-\beta^2-2\beta^4)z^3)\\
&+s^3(1-\beta^2)(4(1+\beta^4)\beta-(5-22\beta^2+9\beta^4-8\beta^6)z\\
&-4(1-2\beta^2-\beta^4)\beta z^2\\
&+(3-4\beta^2+3\beta^4-2\beta^6)z^3)\big]C_0^W\\
&-\frac{1}{4s(1+\beta z)(1+\beta^2+2\beta z)}\\
&\times\big[\big(16m_b^2\big(m_b^2-m_\mathrm{W}^2\big)-4m_\mathrm{W}^2s(1-\beta^2)\big)\\
&\times\beta(\beta+z)(1-3\beta^2+(1-2\beta^2)\beta z+2\beta^2z^2+\beta^3z^3)\\
&-8m_b^2s(1-6\beta^2+3\beta^6+(2-16\beta^2+7\beta^4+2\beta^6)\beta z\\
&+(4-9\beta^2+3\beta^4)\beta^2z^2+(9-4\beta^2-\beta^4)\beta^3z^3\\
&+2(3-\beta^2)\beta^4z^4+\beta^5z^5)\\
&-s^2(1+\beta^2+2\beta z)(1-\beta^2)\\
&\times(2-5\beta^2+\beta^4+(1-2\beta^2-2\beta^4)\beta z\\
&+(3-2\beta^2)\beta^2z^2+(2+\beta^2)\beta^3z^3+\beta^4z^4)\big]\overline{B}_0^W(z)\\
&-\frac{1}{8s}\big[64m_b^6(1+\beta z)-16m_b^4\big(8m_\mathrm{W}^2(1+\beta z)\\
&-s(1-\beta^2-(3-\beta^2)\beta z-2\beta^2z^2)\big)\\
&+m_b^2\big(32\big(2m_\mathrm{W}^4+m_\mathrm{W}^2s(1+\beta z)\big)(1+\beta z)\\
&+4s^2(3-4\beta^4z^2+9\beta z-\beta^5z+2\beta^3z^3\\
&+10\beta^2z^2-2\beta^3z-2\beta^2+\beta^4)\big)\\
&+16m_\mathrm{W}^4s(1-\beta^2)(1+\beta z)\\
&+8m_\mathrm{W}^2s^2\beta(1-\beta^2)(\beta+z)(1+\beta z)\\
&+s^3(1-\beta^2)(1+\beta z)\\
&\times(3-2\beta^2+\beta^4+2(1+\beta^2)\beta z+2\beta^2z^2)\big]C_0^W(z)\\
&-\frac{1}{32s}\big[256m_b^8-128m_b^6\big(6m_\mathrm{W}^2+s\beta z(2+\beta z)\big)\\
&-64m_\mathrm{W}^6s(1-\beta^2)\\
&+32m_b^4\big(24m_\mathrm{W}^4+2m_\mathrm{W}^2s(3+\beta^2+8\beta z+2\beta^2z^2)
\end{aligned}
$$

$$
\begin{aligned}
&- s^2(-3\beta^2+\beta^4+1+2\beta^4z^2\\
&-5\beta^2z^2-6\beta z+2\beta^3z)\big)\\
&-16m_{\mathrm{W}}^4s^2(1-\beta^2)(1+3\beta^2+4\beta z)\\
&-8m_b^2\big(32m_{\mathrm{W}}^6+16m_{\mathrm{W}}^4s(1+\beta^2+2\beta z)\\
&+2m_{\mathrm{W}}^2s^2(5+\beta^4+12\beta z+2(2+\beta^2)\beta^2z^2)\\
&+s^3(4\beta^3z-4\beta^4z^2+\beta^6z^2-2\beta^5z+6\beta^2-2\\
&+4\beta z+2\beta^3z^3+9\beta^2z^2-2\beta^4)\big)\\
&-4m_{\mathrm{W}}^2s^3(1-\beta^2)(3+3\beta^4+4(1+2\beta^2)\beta z+6\beta^2z^2)\\
&-s^4(1-\beta^2)(1+\beta^2+2\beta z)\\
&\times(3-2\beta^2+\beta^4+2(1+\beta^2)\beta z+2\beta^2z^2)\big]D_0^W(z)\Big\}\\
&+(z\to-z)\,, \qquad \text{(B.14)}
\end{aligned}
$$

$$
\begin{aligned}
\frac{\mathrm{d}\sigma_H^{\square}}{\mathrm{d}z} =& -\frac{\alpha}{4\pi}\sigma_0 g_{\mathrm{W}}^2\frac{m_t^2}{m_{\mathrm{W}}^2}\frac{N^2(1-\beta z)-2}{N(1-\beta^2z^2)}\Big\{\beta z(1-z^2)\\
&-\frac{4\beta(1-z^2)(4\beta-z-2\beta z^2)}{s(1+\beta^2+2\beta z)}\big(\overline{A}_0\big(m_t^2\big)-\overline{A}_0\big(m_H^2\big)\big)\\
&+\frac{1}{s\beta}\big[2m_H^2z(5-4\beta^2-(3-2\beta^2)z^2)\\
&-s\beta(2-(7-8\beta^2)\beta z-2z^2+(3-4\beta^2)\beta z^3)\big]\overline{B}_0^t\\
&+\frac{1}{s\beta(1+\beta z)}\big[2m_H^2(-6\beta^3-(5-8\beta^2+4\beta^4)z\\
&-(5-12\beta^2)\beta z^2+(3-4\beta^2+2\beta^4)z^3\\
&+(3-4\beta^2)\beta z^4)\\
&+2s\beta(1-\beta^2)(2+3\beta^2-(3-4\beta^2)\beta z\\
&-(1+6\beta^2)z^2+(1-2\beta^2)\beta z^3+2\beta^2z^4)\big]\overline{B}_0^H\\
&-\frac{1}{s}\big[8m_H^4-4m_H^2s(2-3\beta^2-\beta z)\\
&+s^2(6-10\beta^2+5\beta^4-2(1-2\beta^2)\beta z+\beta^2z^2)\big]C_0^t\\
&+\frac{1}{s\beta}\big[2m_H^4z(5-8\beta^2-(3-2\beta^2)z^2)\\
&-2m_H^2s\beta(1+\beta^2-2(5-6\beta^2)\beta z\\
&-(1-\beta^2)z^2+3(1-\beta^2)\beta z^3)\\
&+s^2\beta^2(\beta-2\beta^3-(7-13\beta^2+8\beta^4)z\\
&+(1-2\beta^2)\beta z^2-2(1-\beta^2)\beta^2z^3)\big]C_0^H\\
&+\frac{1}{s(1+\beta z)(1+\beta^2+2\beta z)}\big[-4m_H^2\beta(\beta+z)\\
&\times(1-3\beta^2+(1-2\beta^2)\beta z+2\beta^2z^2+\beta^3z^3)\\
&-2s(1-3\beta^6+(2+2\beta^2-5\beta^4-4\beta^6)\beta z\\
&+(1+3\beta^2-6\beta^4)\beta^2z^2\\
&+2(1+\beta^2)\beta^5z^3+4\beta^6z^4+\beta^5z^5)\big]\overline{B}_0^H(z)\\
&+\frac{1}{s}\big[\big(8m_H^4-4m_H^2s(2-3\beta^2-\beta z)\big)(1+\beta z)\\
&+s^2(6-10\beta^2+5\beta^4+(3-4\beta^2+4\beta^4)\beta z\\
&-(1-4\beta^2)\beta^2z^2+\beta^3z^3)\big]C_0^H(z)\\
&+\frac{1}{2s}\big[-16m_H^6+16m_H^4s(1-2\beta^2-\beta z)\\
&-2m_H^2s^2(6-13\beta^2+10\beta^4-6(1-2\beta^2)\beta z\\
&+(2+\beta^2)\beta^2z^2)\\
&-s^3(2+\beta^2-6\beta^4+4\beta^6+(5-10\beta^2+8\beta^4)\beta z\\
&+(1+2\beta^2)\beta^4z^2+\beta^3z^3)\big]D_0^H(z)\Big\}+(z\to-z)\,.
\end{aligned}
\qquad \text{(B.15)}
$$

References

1. P. Nason, S. Dawson, R.K. Ellis, Nucl. Phys. B **303**, 607 (1988)
2. P. Nason, S. Dawson, R.K. Ellis, Nucl. Phys. B **327**, 49 (1989)
3. W. Beenakker et al., Phys. Rev. D **40**, 54 (1989)
4. W. Beenakker et al., Nucl. Phys. B **351**, 507 (1991)
5. W. Bernreuther et al., Phys. Rev. Lett. **87**, 242 002 (2001) [hep-ph/0107086]
6. E. Laenen, J. Smith, W.L. van Neerven, Nucl. Phys. B **369**, 543 (1992)
7. N. Kidonakis, J. Smith, Phys. Rev. D **51**, 6092 (1995) [hep-ph/9502341]
8. E.L. Berger, H. Contopanagos, Phys. Rev. D **54**, 3085 (1996) [hep-ph/9603326]
9. S. Catani et al., Nucl. Phys. B **478**, 273 (1996) [hep-ph/9604351]
10. E.L. Berger, H. Contopanagos, Phys. Rev. D **57**, 253 (1998) [hep-ph/9706206]
11. M. Cacciari et al., JHEP **04**, 068 (2004) [hep-ph/0303085]
12. W. Bernreuther et al., Nucl. Phys. B **690**, 81 (2004) [hep-ph/0403035]
13. J.H. Kühn, A.A. Penin, V.A. Smirnov, Eur. Phys. J. C **17**, 97 (2000) [hep-ph/9912503]
14. J.H. Kühn et al., Nucl. Phys. B **616**, 286 (2001) [hep-ph/0106298]
15. A. Denner, S. Pozzorini, Eur. Phys. J. C **18**, 461 (2001) [hep-ph/0010201]
16. A. Denner, S. Pozzorini, Eur. Phys. J. C **21**, 63 (2001) [hep-ph/0104127]
17. J.H. Kühn et al., Phys. Lett. B **609**, 277 (2005) [hep-ph/0408308]
18. J.H. Kühn et al., Nucl. Phys. B **727**, 368 (2005) [hep-ph/0507178]
19. J.H. Kühn et al., JHEP **03**, 059 (2006) [hep-ph/0508253]
20. W. Beenakker et al., Nucl. Phys. B **411**, 343 (1994)
21. C. Kao, D. Wackeroth, Phys. Rev. D **61**, 055 009 (2000) [hep-ph/9902202]
22. J.H. Kühn, A. Scharf, P. Uwer, Eur. Phys. J. C **45**, 139 (2006) [hep-ph/0508092]
23. W. Bernreuther, M. Fücker, Z.G. Si, Phys. Lett. B **633**, 54 (2006) [hep-ph/0508091]
24. S. Moretti, M.R. Nolten, D.A. Ross, hep-ph/0603083
25. G. Passarino, M. Veltman, Nucl. Phys. B **160**, 151 (1979)
26. A. Denner, Fortschr. Phys. **41**, 307 (1993)
27. M. Jezabek, J.H. Kühn, Prepared for the Workshop on e^+e^- Collisions, Hamburg, Germany, 2–3 April 1993
28. W. Bernreuther, M. Fücker, Z.G. Si, hep-ph/0610334
29. S. Kretzer et al., Phys. Rev. D **69**, 114 005 (2004) [hep-ph/0307022]
30. R. Bonciani et al., Nucl. Phys. B **529**, 424 (1998) [hep-ph/9801375]
31. G.J. van Oldenborgh, J.A.M. Vermaseren, Z. Phys. C **46**, 425 (1990)
32. G.J. van Oldenborgh, Comput. Phys. Commun. **66**, 1 (1991)